cmgh
CELLULAR AND MOLECULAR GASTROENTEROLOGY AND HEPATOLOGY

ORIGINAL RESEARCH

Deubiquitinase Josephin Domain-containing Protein 2 Promotes Acute Pancreatitis by Removing K63-linked Poly-ubiqutin Chain on Proliferating Cell Nuclear Antigen in Pancreatic Acinar Cells

Yi Fang,[1,*] Xiang Hu,[2,*] Lijun Ji,[1] Jiaxi Ye,[1] Yaqian Cui,[1] Yongqiang Xiong,[1] Tianyang Jing,[1] Qingsong Zheng,[1] Guang Liang,[1,3] Xin Liu,[4,5] and Wu Luo[1,3]

[1]Medical Research Center, the First Affiliated Hospital, Wenzhou Medical University, Wenzhou, China; [2]Department of Endocrine and Metabolic Diseases, The First Affiliated Hospital of Wenzhou Medical University, Wenzhou, China; [3]School of Pharmaceutical Sciences, Hangzhou Medical College, Hangzhou, Zhejiang, China; [4]Department of Pharmacy and Institute of Inflammation, Zhejiang Provincial People's Hospital, Affiliated People's Hospital of Hangzhou Medical College, Hangzhou, Zhejiang, China; and [5]Department of Colorectal Surgery, Zhejiang Provincial People's Hospital, Affiliated People's Hospital of Hangzhou Medical College, Hangzhou, Zhejiang, China

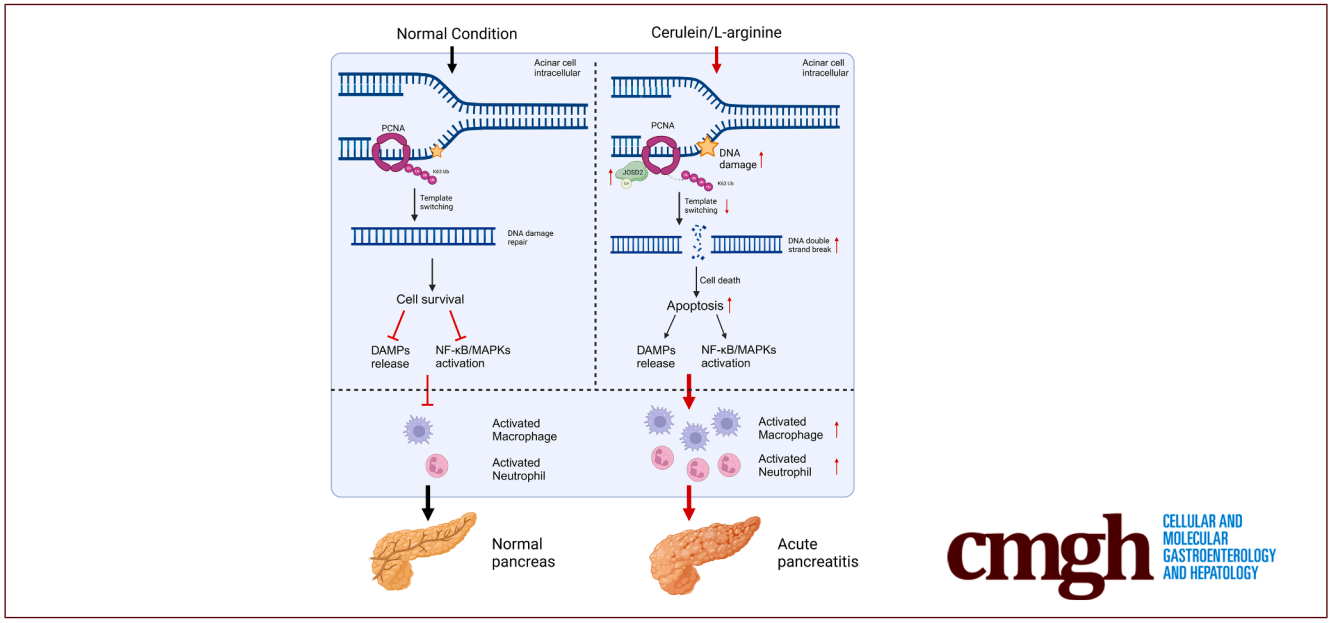

SUMMARY

Josephin domain-containing protein 2 is upregulated in response to pancreatic injury and plays a significant role in different acute pancreatitis mouse models. This study reveals that Josephin domain-containing protein 2 deubiquitinates proliferating cell nuclear antigen and inhibits its DNA damage repair function, promoting acinar cell death during acute pancreatitis.

BACKGROUND & AIMS: Acute pancreatitis (AP) results in localized pancreatic injury or systemic inflammatory responses, contributing to high morbidity and mortality worldwide. Acinar cell death and inflammation are critical key drivers of AP progression. Some deubiquitinases (DUBs), which regulate the stability and/or activity of substrate proteins, may play a role in the development of AP. Here, we aimed to investigate how Josephin domain-containing protein 2 (JOSD2) involved in AP progression.

METHODS: JOSD2 expression was assessed in mouse pancreatic tissues with cerulein-induced AP. Cerulein- or L-arginine-induced AP models were constructed in whole-body JOSD2 knockout (JOSD2$^{-/-}$) and wild-type (WT) mice. Bone marrow JOSD2$^{-/-}$ chimeric mice were generated and subjected to cerulein-induced AP. In vitro studies were conducted on primary acinar cells isolated from JOSD2$^{-/-}$ and WT mice.

RESULTS: JOSD2 expression was upregulated in the pancreas of cerulein-treated mice, and the loss of JOSD2 offered protection against cerulein- or L-arginine-induced AP. Bone marrow transplantation assay revealed that myeloid JOSD2 was not involved in the progression of cerulein-induced AP. In vitro studies, primary acinar cells isolated from JOSD2$^{-/-}$ mice demonstrated increased resistance to cerulein-induced injury and inflammation. Proliferating cell nuclear antigen (PCNA) was identified as a key substrate of JOSD2. JOSD2 selectively removes K63-linked polyubiquitin chains from PCNA at the K164 site. The protective effects of JOSD2 deficiency on DNA damage and acinar cell death were reversed by the PCNA inhibitor PCNA-I1.

CONCLUSIONS: JOSD2 regulates AP progression via PCNA-mediated DNA damage response and may serve as a promising therapeutic target for AP treatment. *(Cell Mol Gastroenterol Hepatol 2025;19:101621; https://doi.org/10.1016/j.jcmgh.2025.101621)*

Keywords: Acinar Cells; Acute Pancreatitis; Deubiqutination; JOSD2; PCNA.

Acute pancreatitis (AP) is a life-threatening digestive disease characterized by pancreatic self-digestion, often due to the premature activation of pancreatic trypsinogen and subsequent inflammation of the pancreas.[1,2] Several risk factors, such as pancreatic ductal obstruction, alcohol abuse, smoking, obesity, and drug toxicity, contribute to the increasing incidence of AP.[3] Although most cases of AP are mild and self-limiting, approximately 20% progress to severe acute pancreatitis (SAP), which is associated with serious complications, poor prognosis, and high mortality.[4] Additionally, acute lung injury (ALI) is a major extrapancreatic complication resulting from AP.[5] Despite advancements in diagnosis and treatment strategies, clinical management of AP remains limited to supportive therapy.[6] Thus, understanding the pathogenesis of AP is essential for developing specific and effective therapies for clinical use.

As the predominant cell type in the exocrine pancreas, acinar cells are responsible for synthesizing, storing, and secretion of various digestive enzymes.[7,8] Acinar cell injury, resulting from the premature activation of pancreatic zymogens, is considered the initial stage of AP and plays a critical role in its progression.[9,10] This early activation of pancreatic proteases leads to acinar cell damage and the initiation of inflammatory pathways, followed by the release of endogenous molecules and inflammatory cytokines.[11,12] Subsequently, immune cells such as macrophages and neutrophils are recruited to the pancreas, where they further secrete cytokines and chemokines, amplifying the inflammatory response and exacerbating disease progression.[8,11] Based on this understanding, preventing acinar cell injury and controlling the inflammatory response are key therapeutic strategies for AP management.

Ubiquitination is recognized as one of the most important post-translational modifications (PTMs) involved in the progression of various human diseases.[13] E3 ubiquitin ligases and deubiquitinases (DUBs) regulate the stability and activity of substrate proteins, which is essential for various pathological processes, by adding and removing ubiquitin, respectively.[14,15] Several DUBs have been implicated in the pathogenesis of AP. For example, tumor necrosis factor alpha-induced protein 3 (TNFAIP3, also known as A20) promotes receptor-interacting protein 3 (RIP3) phosphorylation through deubiquitination, which activates the NLRP3 inflammasome and exacerbates sodium taurocholate-induced AP in rats.[16] Moreover, our team and others has shown that ubiquitin-specific protease 25 (USP25) deficiency significantly aggravates pancreatic injury and inflammation by facilitating tank-binding kinase 1 (TBK1)-nuclear factor-κB (NF-κB)[17] and signal transducer and activator of transcription 3 (STAT3)[18] signaling pathways. Josephin domain-containing protein 2 (JOSD2), a member of the Machado-Joseph domain (MJD)-containing protease family—the smallest subfamily of DUBs—contains a highly conserved cysteine protease domain known as the Josephin domain, found throughout all eukaryotes.[19,20] Previous studies have demonstrated that JOSD2 physically interacts with YAP/TAZ, preventing their ubiquitin-dependent degradation and thus promoting cholangiocarcinoma (CCA) cell proliferation and malignant tumor progression.[21] Additionally, JOSD2 deubiquitinates and stabilizes 3 key glycolytic enzymes (aldolase A, phosphofructokinase-1 and phosphoglycerate dehydrogenase), facilitating glycolysis and lung adenocarcinoma progression.[22] First, our recent studies found that JOSD2 act as an protective factor in Angiotensin II (AngII)-induced cardiac hypertrophy and vascular remodeling by stabilizing SMAD7 in vascular smooth muscle cell[23] and SERCA2a in cardiomyocytes,[24] respectively. Second, our team reported that JOSD2 mediated severe calcium mishandling in isoproterenol (ISO)-induced cardiac hypertrophy by deubiquitinating CaMKIIδ in cardiomyocytes.[25] Finally, our lab demonstrated that JOSD2 alleviates colitis and acute kidney injury by inhibiting NF-κB inflammatory pathway via deubiquitination of IMPDH2 in macrophages[26] and SIRT7 in renal tubular epithelial cells,[27] respectively. However, the role of JOSD2 in AP, particularly in relation to acinar cell death and inflammation, remains largely unknown.

This study aimed to investigate the impact of JOSD2 on pancreatic injury in AP. Our findings revealed that the expression of JOSD2 is markedly increased in AP and JOSD2 knockout alleviated pancreatic injury and inflammation in

***Author share co-first authorship.**

Abbreviations used in this paper: **ALI, acute lung injury; Ang II, Angiotensin II; ANOVA, analysis of variance; AP, acute pancreatitis; BMDM, bone marrow-derived macrophage; BSA, bovine serum albumin; CBS, cysthionine-β-synthase; CCA, cholangiocarcinoma; CER, cerulein; Cle, cleaved; co-IP, co-immunoprecipitation; DAMPs, damage-associated molecular patterns; DDT, DNA damage tolerance; DMEM, Dulbecco's modified Eagle medium; DSBs, double-strand breaks; DUBs, deubiquitinases; ELISA, enzyme-linked immunosorbent assay; FBS, fetal bovine serum; GAPDH, glyceraldehyde-3-phosphate dehydrogenase; gDNA, genomic DNA; GSH, glutathione; H&E, hematoxylin and eosin; HRP, horseradish peroxidase; IL, interleukin; ISO, isoproterenol; JOSD2, Josephin domain-containing protein 2; KO, knockout; LC-MS/MS, liquid chromatography-tandem mass spectrometry; LDH, lactate dehydrogenase; LFQ, Lock Forming Quality; MAPKS, mitogen-activated protein kinases; MJD, Machado-Joseph domain; MPO, myeloperoxidase; MW, molecular weight; NF-κB, nuclear factor-κB; PBS, phosphate buffered saline; PCNA, proliferating cell nuclear antigen; PCNA-I1, PCNA inhibitor 1; PTM, post-translation modification; PVDF, polyvinylidene difluoride; RIP3, receptor-interacting protein 3; ROS, reactive oxygen species; RT-qPCR, real-time quantitative polymerase chain reaction; SAP, severe acute pancreatitis; SBTI, soybean trypsin inhibitor; SD, standard deviation; SDS-PAGE, sodium dodecyl sulfate-polyacrylamide gel electrophoresis; STAT3, signal transducer and activator of transcription 3; TBK1, tank-binding kinase 1; TLS, translesion synthesis; TMB, 3,3′,5,5′-trimethylbenzidine; TNF-α, tumor necrosis factor-α; TNFAIP3, tumor necrosis factor alpha-induced protein 3; TS, template switching; USP25, ubiquitin-specific protease 25; WT, wild-type.**

Most current article

2352-345X
https://doi.org/10.1016/j.jcmgh.2025.101621

in vivo and in vitro models. To further explore the specific role of myeloid-derived JOSD2 in AP, myeloid-specific JOSD2 knockout chimera mice were constructed via bone marrow transplantation. Interestingly, the deletion of JOSD2 in myeloid cells had no impact on the progression of AP. This suggests that JOSD2 expression in acinar cells is primarily responsible for driving the disease progression. Mechanistically, it was found that JOSD2 deubiquitinates K63-linked ubiquitin chains from the K164 site of proliferating cell nuclear antigen (PCNA), which subsequently inhibits DNA damage repair and promotes cell death in acinar cell. These findings establish JOSD2 as a key regulator of AP, highlighting its potential as a novel therapeutic target for treating this disease.

Results

JOSD2 Deficiency Mitigates Single Cerulein Cycle-induced AP

To determine whether JOSD2 plays a role in the pathogenesis of AP, we measured JOSD2 expression levels in pancreatic tissues from wild-type (WT) mice treated with either single Cerulein (CER) cycle or saline (Figure 1*A*). Both protein and mRNA levels of JOSD2 were significantly elevated in the CER-induced AP group (Figure 1*B–D*). To further explore the potential role of JOSD2 in experimental AP, WT and whole-body JOSD2 knockout (KO) mice ($JOSD2^{-/-}$) were used, which were similarly administered 50 μg/kg CER (8 consecutive injections, 1 per hour). Compared with WT mice, $JOSD2^{-/-}$ mice exhibited reduced pancreatic edema during AP, as evidenced by gross pancreatic appearance and the pancreas weight-to-body weight ratio (Figure 1*E–F*). Additionally, common biochemical markers for AP (such as pancreatic trypsin activities and serum levels of amylase, lipase, and lactate dehydrogenase [LDH]) showed that JOSD2 deficiency significantly attenuated CER-induced pancreatic dysfunction (Figure 1*G*). Histopathological analysis, including hematoxylin and eosin (H&E) staining and scoring, further confirmed that JOSD2 KO mice were protected against CER-induced pancreatic edema, inflammatory infiltration, and necrosis (Figure 1*H–I*). Overall, JOSD2 deficiency effectively inhibited pancreatic injury in a single CER cycle-induced AP model.

JOSD2 Deficiency Reduces Single CER Cycle-induced Local and Systemic Inflammation

Given the pivotal role of inflammation in AP progression,[8] both local and systemic inflammatory responses were evaluated in CER-challenged WT and $JOSD2^{-/-}$ mice. As anticipated, JOSD2 KO significantly reduced serum levels of the inflammatory cytokines interleukin (IL)-6 and tumor necrosis factor-α (TNF-α) in response to CER-induced AP, compared with WT mice (Figure 2*A*). Similarly, both protein and mRNA levels of IL-6 and TNF-α were notably lower in pancreatic tissues from $JOSD2^{-/-}$ mice relative to WT mice (Figure 2*B–C*). Moreover, myeloperoxidase (MPO) activity, a marker of neutrophil infiltration, was significantly reduced in the pancreas and lungs of $JOSD2^{-/-}$ mice during AP (Figure 2*D*). F4/80 and MPO staining, markers of macrophages and neutrophils/monocytes, respectively, further confirmed that inflammatory cell infiltration in the pancreas was significantly alleviated in $JOSD2^{-/-}$ mice (Figure 2*E–F*). Mitogen-activated protein kinases (MAPKs) and NF-κB signaling pathways are known to regulate inflammatory responses and contribute to AP progression.[28,29] As shown in Figure 2*G–H*, JOSD2 deficiency significantly inhibited the phosphorylation of ERK, JNK, and p65, as well as the degradation of IκB in the pancreas following Cerulein treatment. Systemic inflammation in AP often leads to multi-organ failure, including ALI.[4,30] Histological examination of lung tissue via H&E staining revealed that $JOSD2^{-/-}$ mice exhibited less structural lung damage compared with WT mice after CER administration (Figure 3*A*). Additionally, immunohistochemistry staining showed that the recruitment of macrophages and neutrophils into lung tissue was significantly reduced in $JOSD2^{-/-}$ mice (Figure 3*B–C*).

JOSD2 Deficiency Relieves Multiple CER Cycle-induced Severe AP and Inflammation in Mice

Meanwhile, we evaluated the protective effects of JOSD2 KO on prolonged hyperstimulation CER (8 injections on 3 consecutive days) (Figure 4*A*). Multiple CER administration over several days presented more severe AP. Consistent with previous results, both protein and mRNA levels of JOSD2 were significantly upregulated in the multiple CER cycle-induced AP group (Figure 4*B–D*). JOSD2 KO significantly inhibited pancreatic and lung dysfunction under CER stimulation (Figure 4*E–I*). Moreover, JOSD2 deficiency alleviates macrophage infiltration and inflammatory response in multiple CER cycle-induced AP (Figure 4*H, J–K*). In conclusion, $JOSD2^{-/-}$ mice showed a significantly attenuated pancreatic injury and inflammatory response upon prolonged hyperstimulation of CER.

JOSD2 Deficiency Protects Against L-arginine-induced AP

To further examine the role of JOSD2 in other experimental models of AP, severe AP was induced in WT and $JOSD2^{-/-}$ mice via intraperitoneal injection of L-arginine (Figure 5*A*). The results showed that $JOSD2^{-/-}$ mice exhibited a significantly higher survival rate compared with WT mice treated with L-arginine (Figure 5*B*). Gross pancreatic appearance (Figure 4*B*) and pancreas-to-body weight ratios (Figure 5*D*) indicated edema after L-arginine injections, which was less severe in the $JOSD2^{-/-}$ mice compared with the WT mice. Pancreatic injury markers, including intrapancreatic trypsin activation, serum amylase, lipase, and LDH levels, indicated that JOSD2 deficiency led to significantly reduced pancreatic injury in the L-arginine-induced AP model (Figure 5*E–G*). Histopathological analyses further corroborated these findings, showing that $JOSD2^{-/-}$ mice displayed only mild damage to the exocrine pancreas and lung tissues compared with WT mice (Figure 5*H–I*). Immunohistochemical analysis using an anti-F4/80 antibody demonstrated a significant reduction in macrophage infiltration into the pancreas and lungs of

JOSD2$^{-/-}$ mice during L-arginine-induced AP (Figure 5*J*–*K*). Additionally, the relative mRNA expression levels of pro-inflammatory cytokines *Il6* and *Tnf* in the pancreas were significantly lower in JOSD2$^{-/-}$ mice than in WT mice (Figure 5*L*). These findings suggest that JOSD2 deficiency alleviates pancreatic injury and reduces the inflammatory response in L-arginine-induced AP, highlighting JOSD2 as a potential target for AP treatment.

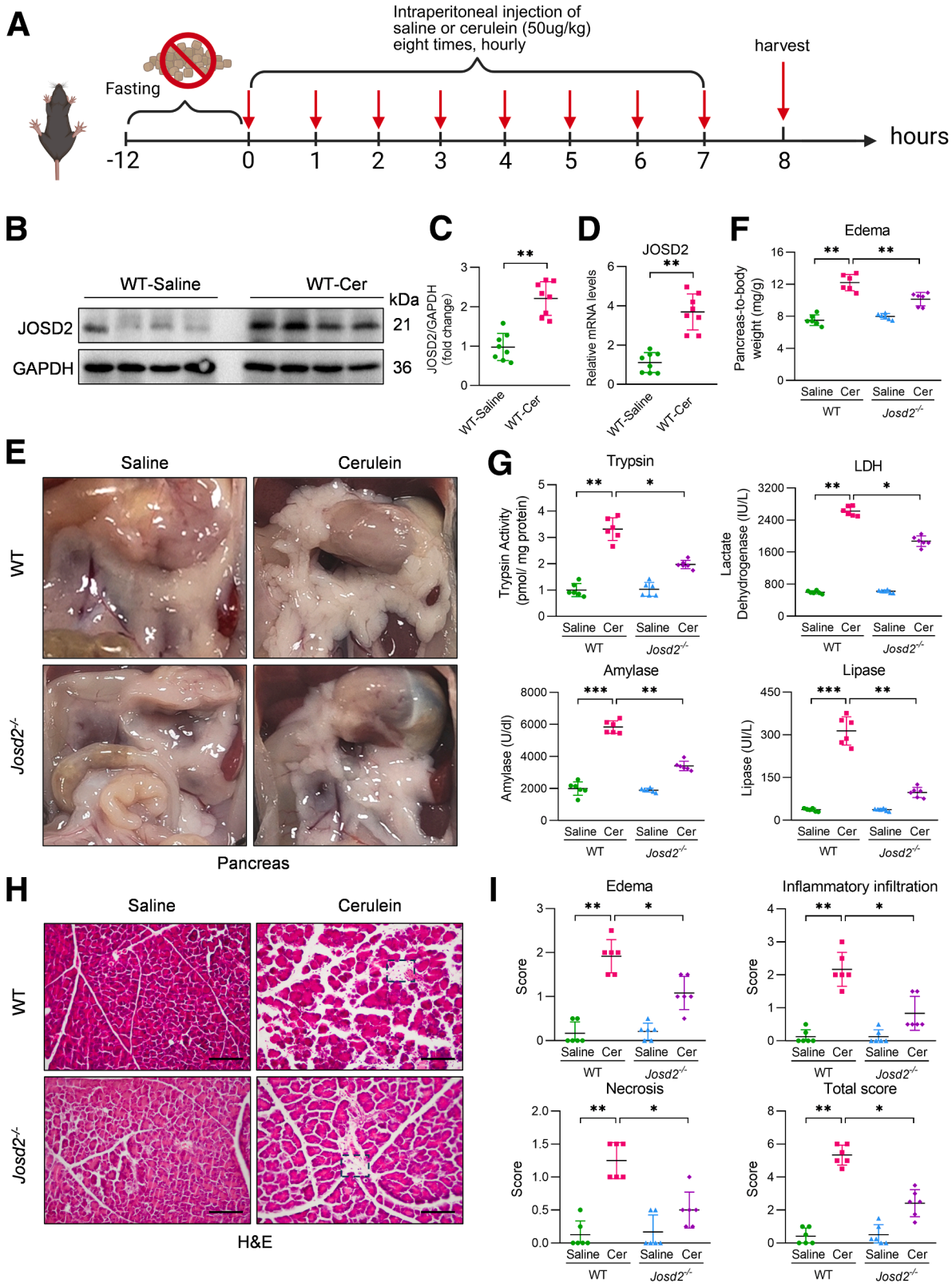

Acinar Cell JOSD2 Plays a Dominant Role in Mediating CER-induced AP

Pancreatic acinar cell injury and immune cell infiltration play crucial roles in the progression of AP.[8,9] Considering that pancreatic immune cells are mainly derived from bone marrow,[31,32] bone marrow chimeric mice were constructed through bone marrow transplantation to determine whether JOSD2 in myeloid cells contributes to AP. WT mice were irradiated to deplete endogenous bone marrow and were subsequently reconstituted with bone marrow cells from either WT or JOSD2$^{-/-}$ donor mice (Figure 6*A*). The efficiency of bone marrow transplantation was confirmed through Western blot and real time quantitative polymerase chain reaction (RT-qPCR) analyses (Figure 6*B*–*C*). Surprisingly, JOSD2 deficiency in myeloid cells did not affect pancreatic injury or histopathological changes in CER-induced AP (Figure 6*D*–*G*). Furthermore, the levels of inflammatory cytokines *Il6* and *Tnf* showed no significant differences, indicating that myeloid cell-specific JOSD2 does not contribute to the inflammatory response during AP (Figure 6*H*).

Given that JOSD2 expression in pancreatic acinar cells is higher than in myeloid cells and acinar cell injury is the initial and critical stage in AP progression,[9] we focused on acinar cell-specific JOSD2. To investigate its role in vitro, acinar cells were isolated from the pancreas of WT and JOSD2$^{-/-}$ mice. Upon CER stimulation, JOSD2$^{-/-}$ acinar cells exhibited less cell injury, cell death, and reduced digestive enzyme release into the culture supernatant compared with WT cells (Figure 7*A*–*B*). Additionally, JOSD2 deficiency in acinar cells significantly reduced mRNA levels of inflammatory cytokines *Il6* and *Tnf* and lowered protein levels of IL-6 and TNF-α in the supernatant (Figure 7*C*–*D*). Furthermore, the activation of MAPK and NF-κB signaling pathways, which are key mediators of inflammation, was significantly enhanced in WT acinar cells treated with CER but was markedly inhibited in JOSD2$^{-/-}$ acinar cells (Figure 7*E*–*F*). Taken together, these findings demonstrate that JOSD2 in pancreatic acinar cells plays a dominant role in regulating CER-induced pancreatic injury and inflammatory responses, highlighting the significance of acinar cell JOSD2 in the progression of AP.

JOSD2 Directly Interacts With PCNA and Deubiquitinate K63-linked Ubiquitin Chains

As a deubiquitinase, JOSD2 exerts its biological functions by selectively removing ubiquitin from its target substrates. To identify the potential substrates of JOSD2, co-immunoprecipitation (co-IP) followed by liquid chromatography-tandem mass spectrometry (LC-MS/MS) analysis was performed in 293T cells overexpressing JOSD2 (Figure 8*A*; Table 1). Interestingly, PCNA, a key regulator in DNA damage repair during external stress, was identified as a potential target of JOSD2 (Figure 8*B*–*C*). To confirm the interaction between JOSD2 and PCNA, co-IP assays were conducted in 293T cells co-transfected with JOSD2-Flag and PCNA-HA plasmids. The results demonstrated a clear interaction between JOSD2 and PCNA (Figure 8*D*). Co-IP assay showed that CER significantly enhanced the endogenous interaction between JOSD2 and PCNA in pancreas tissues of CER-challenged mice (Figure 8*E*). Furthermore, we also observed an stronger endogenous JOSD2-PCNA complex in CER-stimulated AR42J through a co-IP assay (Figure 8*F*). Previous studies have shown that the ubiquitination of PCNA plays a crucial role in activating DNA damage repair and replication pathways.[33,34] We hypothesized that JOSD2 could directly deubiquitinate PCNA. To explore this hypothesis, 293T cells were cotransfected with PCNA-HA, Ub-Myc, and either JOSD2-Flag or JOSD2-C24A-Flag (a dominant-negative mutant of JOSD2), followed by treatment with MG132 to prevent proteasomal degradation. As expected, JOSD2 significantly removed ubiquitin chains from PCNA in a dose-dependent manner, whereas JOSD2-C24A failed to do so, indicating that JOSD2 directly hydrolyzes ubiquitin chains from PCNA (Figure 8*G*). Because previous reports have demonstrated that members of the MJD family preferentially cleave K48- and K63-linked ubiquitin chains,[19,35] we further examined whether JOSD2 specifically targets these linkages. 293T cells were transfected with Ub-Myc-WT, Ub-Myc-K48O, Ub-Myc-K63O, Ub-Myc-K48R, and Ub-Myc-K63R plasmids. The results showed that JOSD2 selectively downregulated K63-linked ubiquitin chains on PCNA rather than K48-linked ubiquitin chains (Figure 8*H*–*J*). In addition, we detected endogenous K63-ubiquitination of PCNA in AR42J treated with CER and found that CER-induced upregulated JOSD2 caused a significant reduction in PCNA K63-ubiquitination (Figure 8*K*). In contrast, JOSD2 deficiency increased the PCNA K63-ubiquitination in CER-challenged pancreas tissue (Figure 8*L*). Thus, we inferred that JOSD2 directly interacts with PCNA and cleaves its K63-linked ubiquitination.

JOSD2 Mediates Acinar Cell Injury and Death by Regulating PCNA

To explore whether PCNA serves as the key substrate for JOSD2 during pancreatic injury, PCNA-I1, a specific inhibitor

Figure 1. (***See previous page***). **Knockout of JOSD2 reduced the severity of pancreatic injury in the single CER cycle-induced AP model.** (*A*) Schematic illustration of single CER cycle-induced AP model. Immunoblot analysis (*B*) and optical density quantification (*C*) of JOSD2 expression in pancreatic tissues from mice treated with saline or CER. GAPDH was used as the loading control (n = 8). (*D*) RT-qPCR analysis of *JOSD2* mRNA levels in pancreatic tissues of saline or CER-treated WT mice. Data were normalized to GAPDH (n = 8). (*E*) Gross pancreatic images were taken in WT and JOSD2$^{-/-}$ mice following 8 CER injections (n = 6). (*F*) Ratio of pancreas weight to body weight (n = 6). (*G*) Pancreatic trypsin activity, serum amylase, lipase, and LDH levels of WT and JOSD2$^{-/-}$ mice after saline or CER injection (n = 6). (*H*) Representative images of H&E-stained pancreas sections from WT and JOSD2$^{-/-}$ mice after saline or CER stimulation (n = 6). Scale bar: 100 μm. (*I*) Histopathologic scoring of pancreas edema, inflammation infiltration, and necrosis in pancreas tissues (n = 6). All data are shown as means ± SD; $^{*}P < .05$, $^{**}P < .01$, $^{***}P < .001$. All experimental animals were female.

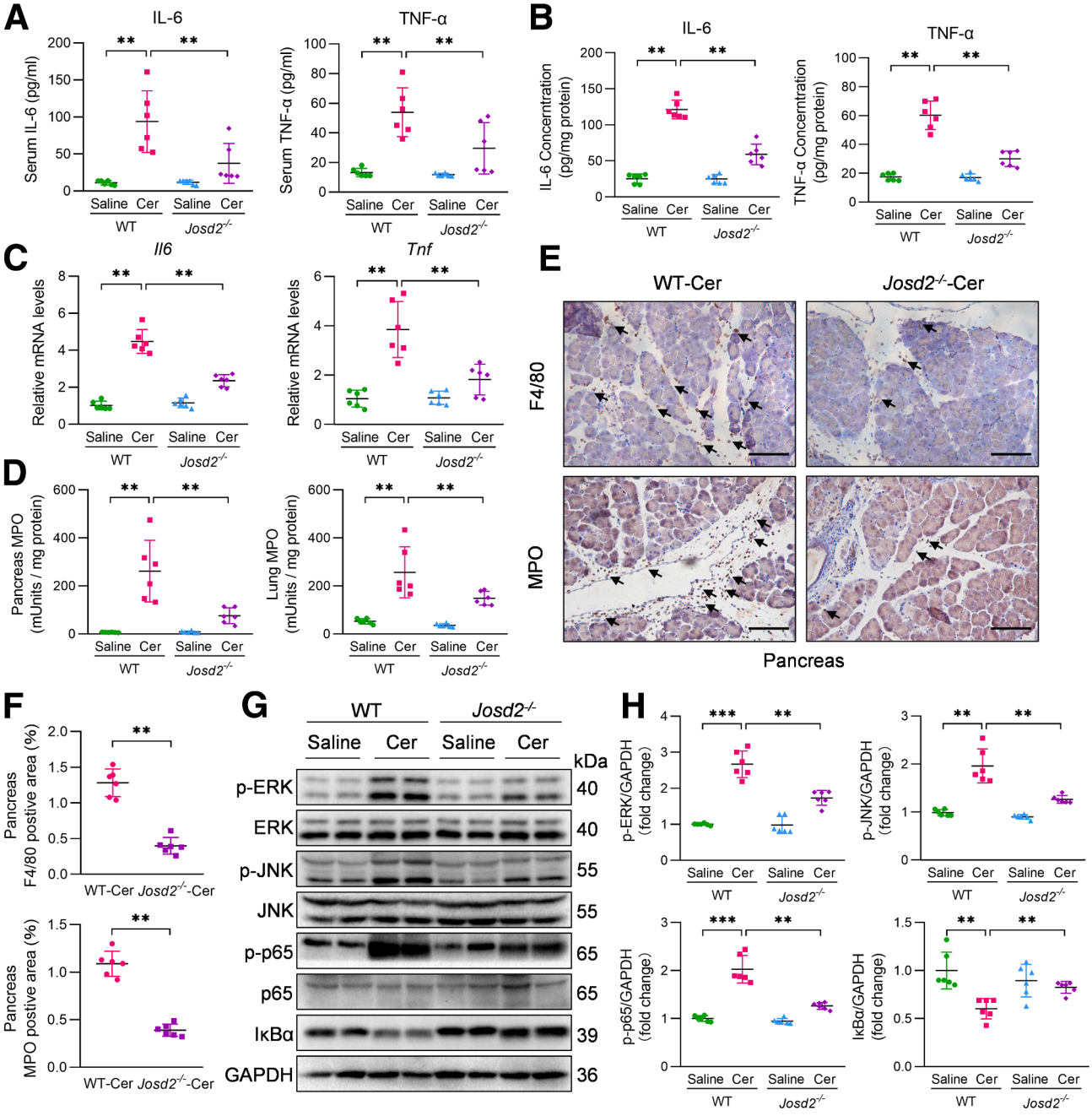

Figure 2. JOSD2$^{-/-}$ mice present less severe pancreas inflammation infiltration in the single CER cycle-induced AP model. Protein concentrations in serum (*A*) and tissues (*B*) of inflammatory cytokines IL-6 and TNF-α from WT and JOSD2$^{-/-}$ mice upon saline or CER treatment (n = 6). (*C*) *Il6* and *Tnf* mRNA levels in pancreas tissues obtained from WT and JOSD2$^{-/-}$after saline or CER administration. Data of mRNA levels were normalized to GAPDH (n = 6). (*D*) MPO activity in the pancreas tissues from the indicated groups was determined (n = 6). Representative immunohistochemistry staining images (*E*) and quantification (*F*) of F4/80 and MPO in pancreas tissue sections (n = 6). *Black arrows* indicate the positive region. Scale bar: 100 μm. (*G*) Western blot analysis of the activity of MAPKs and NF-κB in the pancreas tissues from saline or CER-induced WT and JOSD2$^{-/-}$ mice (n = 6). (*H*) Densitometric quantification of Western blot image shown in panel *G*. GAPDH was used as the loading control. Data are presented as means ± SD; $^{**}P < .01$, $^{***}P < .001$. All experimental animals were female.

of PCNA, was used. PCNA-I1 has been shown to activate the DNA damage response and promote cell death.[36] WT and JOSD2$^{-/-}$ acinar cells were pretreated with PCNA-I1 and subsequently exposed to CER (Figure 9*A*). Interestingly, JOSD2$^{-/-}$ acinar cells treated with PCNA-I1 demonstrated increased susceptibility to CER-induced injury, as indicated by elevated levels of LDH, lipase, and amylase in the supernatant (Figure 9*B*). Furthermore, the levels of both mRNA and secreted pro-inflammatory cytokines (IL-6 and TNF-α) in acinar cells suggested that inhibition of PCNA

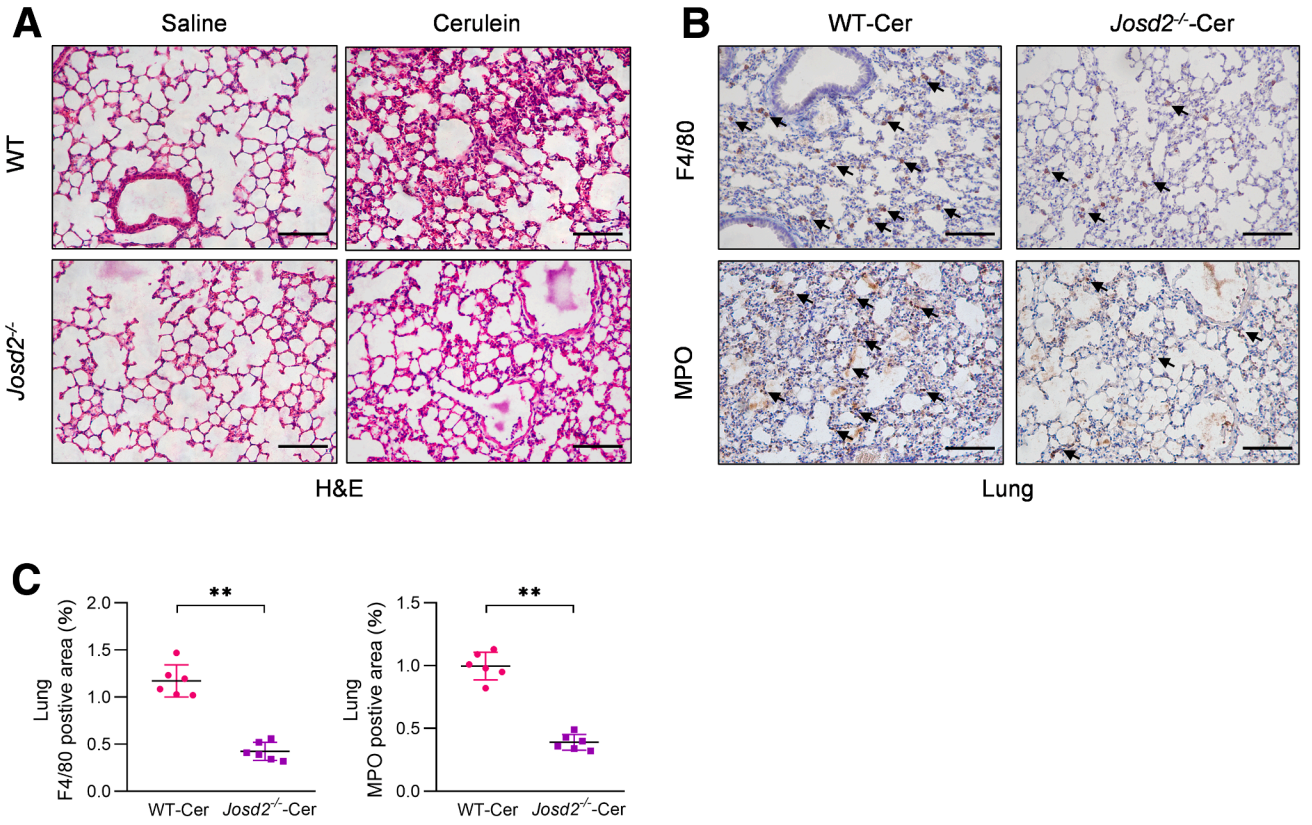

Figure 3. JOSD2 deficiency inhibited single CER cycle-induced AP-associated lung injury induced by CER. (*A*) Representative H&E staining images of lung sections from WT and JOSD2$^{-/-}$ mice treated with CER (n = 6). Scale bar: 100 μm. Immunohistochemistry images (*B*) and corresponding quantification (*C*) of F4/80- and MPO-stained lung sections from WT and JOSD2$^{-/-}$ mice treated with CER (n = 6). *Black arrows* indicate the positive region. Scale bar: 100 μm. Data are shown as means ± SD; $^{**}P < .01$. All experimental animals were female.

counteracted the protective effects conferred by JOSD2 deficiency in CER-induced inflammatory responses (Figure 9*C–D*). Western blot analysis revealed that JOSD2 knockout suppressed CER-induced activation of MAPKs and NF-κB signaling, but this effect was reversed by PCNA-I1 treatment in acinar cells (Figure 9*E–F*). Previous research has shown that CER-induced apoptotic acinar cells release damage-associated molecular patterns (DAMPs), which exacerbate pancreatic injury and inflammation.[28,37] Additionally, the protective effects of JOSD2-knockdown on DNA damage, evidenced by downregulated levels of γ-H2Ax and cleaved PARP (Cle-PARP), were reversed by PCNA-I1 treatment (Figure 9*G–H*). Furthermore, JOSD2 deficiency inhibited the expression of pro-apoptotic proteins, such as cleaved caspase-3 (Cle-caspase3) and Bax, in response to CER stimulation. However, these protective effects were reversed by PCNA-I1 treatment (Figure 9*G–H*). Taken together, these findings suggest that JOSD2 mediates acinar cell injury and death through a PCNA-dependent mechanism during CER-induced AP.

JOSD2 Deubiquitinates PCNA at K164 to Block DNA Damage Repair in Acinar Cells

To determine the specific ubiquitination site on PCNA targeted by JOSD2, PCNA at lysine residues K14, K138, and K164 were potential ubiquitination sites by an online ubiquitination site predicted tool (http://gpsuber.biocuckoo.cn/online.php). The results indicated that JOSD2 significantly reduced the ubiquitination levels in 293T cells expressing expressing PCNA-WT, PCNA-K14R, and PCNA-K138R but had no effect on PCNA-K164R (Figure 10*A*). To further confirm whether the K164 site was required for PCNA activity and downstream DNA damage repair, PCNA-WT and PCNA-K164R expression was rescued in AR42J cells by transfection. Compared with WT, PCNA-K164R promoted the expression of *Il6* and *Tnf* mRNA following CER stimulation (Figure 10*B*). Consistently, the IL-6 and TNF-α levels in the supernatants of CER-stimulated AR42J were dramatically increased by transfection with a PCNA-K164R (Figure 10*C*). Cerulein remarkably triggered MAPKs and NF-κB signaling pathways in AR42J containing PCNA-WT, which was further promoted by PCNA-K164R overexpressed (Figure 10*D–E*). Similarly, PCNA-K164R aggravated the CER-induced DNA damage and pro-apoptotic related protein markers (Figure 10*F–G*). These results suggest that the deubiquitinating modification at K164 of PCNA is responsible for the acinar cell injury. Overall, JOSD2 deubiquitinates PCNA at K164 to block DNA damage repair in acinar cells.

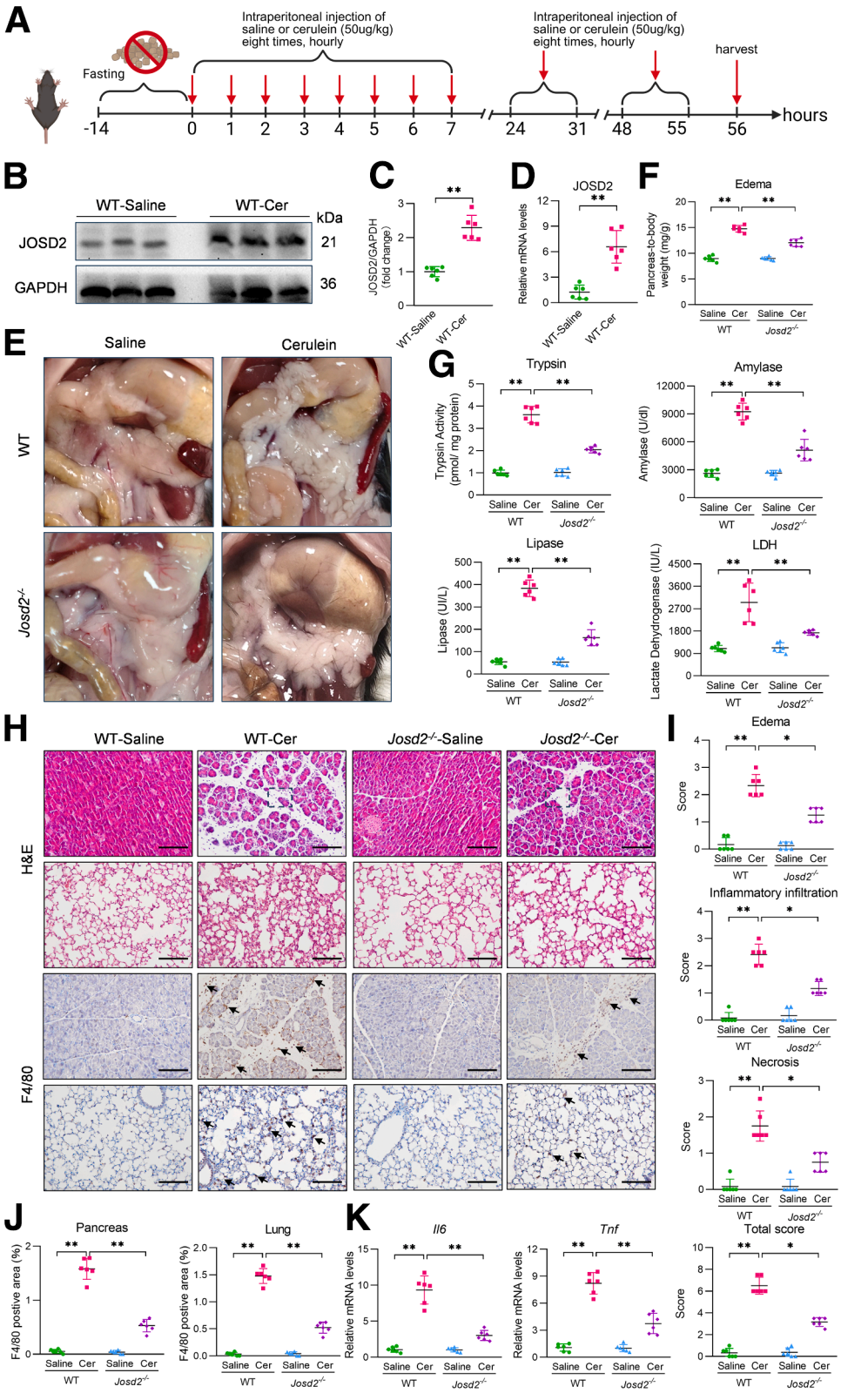

Figure 4. JOSD2 deficiency relieved multiple CER cycle-induced severe AP and inflammation in mice. (*A*) Schematic illustration of a multiple CER cycle-induced AP model. Immunoblot analysis (*B*) and optical density quantification (*C*) of JOSD2 expression in pancreatic tissues from mice treated with saline or multiple CER cycle injections. GAPDH was used as the loading control (n = 6). (*D*) RT-qPCR analysis of JOSD2 mRNA levels in pancreatic tissues of saline or multiple CER cycle-treated WT mice. Data were normalized to GAPDH (n = 6). (*E*) Gross pancreatic images were taken in WT and JOSD2$^{-/-}$ mice following multiple CER cycle injections (n = 6). (*F*) Ratio of pancreas weight to body weight (n = 6). (*G*) Pancreatic trypsin activity, serum amylase, lipase, and LDH levels of WT and JOSD2$^{-/-}$ mice after saline or multiple CER cycle injections (n = 6). (*H*) Representative images of H&E-stained and F4/80-stained pancreas sections from WT and JOSD2$^{-/-}$ mice after saline or multiple CER cycle injections (n = 6). Scale bar: 100 μm. (*I*) Histopathologic scoring of pancreas edema, inflammation infiltration, and necrosis in pancreas tissues (n = 6). (*J*) quantification of F4/80 in pancreas and lung tissue sections (n = 6). (*K*) Il6 and Tnf mRNA levels in pancreas tissues obtained from WT and JOSD2-/-after saline or multiple CER cycle administration. Data of mRNA levels were normalized to GAPDH (n = 6). Data are presented as means ± SD; *$P < .05$, **$P < .01$. All experimental animals were female.

Discussion

AP remains an unpredictable and lethal gastrointestinal disease due to challenges in early diagnosis and the limited availability of effective therapeutic options. To date, no specific treatments exist for AP, and clinical management is primarily supportive, involving fluid resuscitation, analgesia, and nutritional support.[38,39] An increasing number of clinical trials investigating treatment strategies targeting

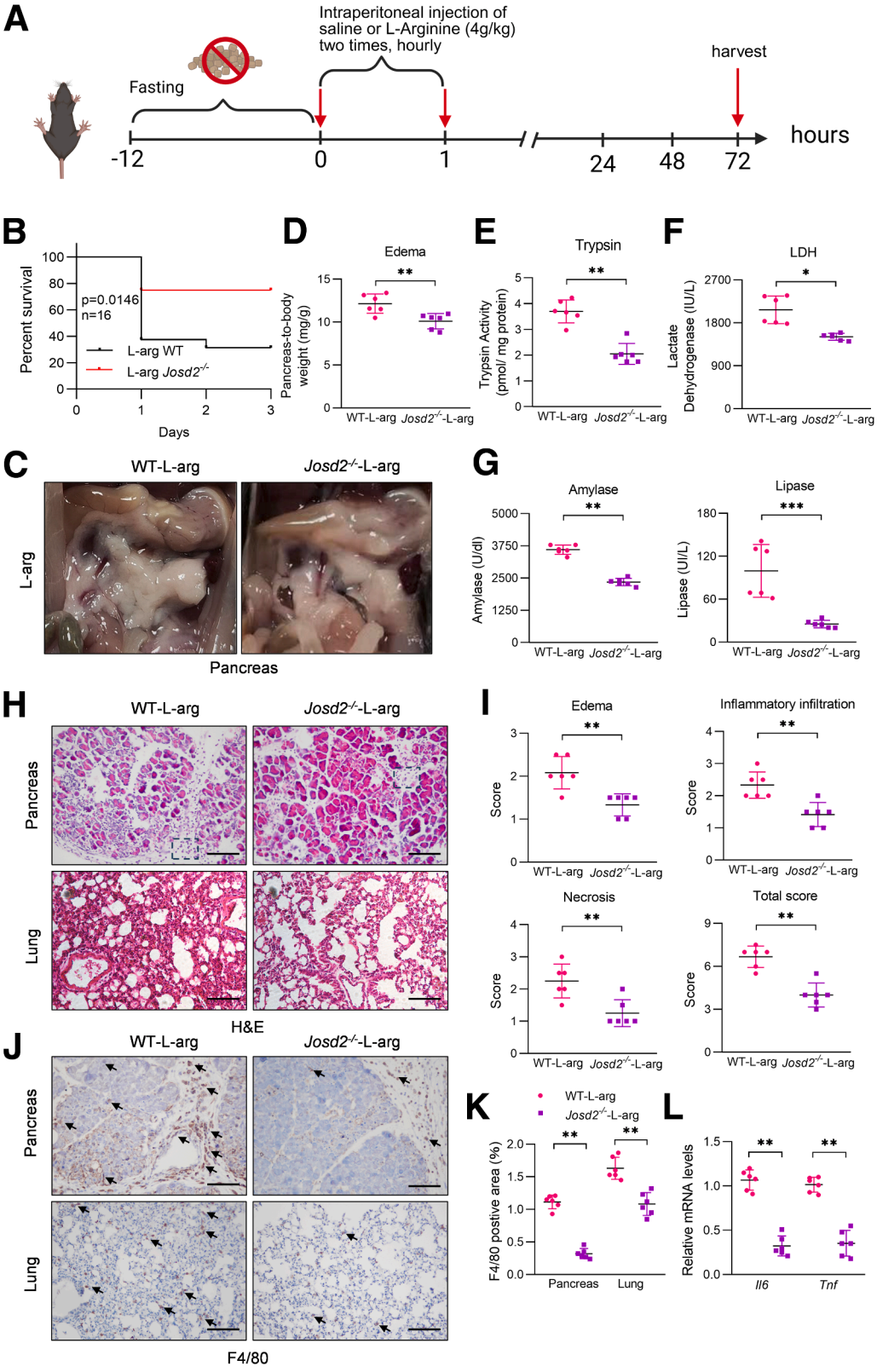

immune responses and calcium channels have been conducted.[40] In the early stage of AP, endogenous and exogenous factors incite initial damage to acinar cells, triggering an inflammatory cascade that increases pancreatic damage and systemic inflammation.[41,42] Reducing initial pancreatic acinar cell death is likely crucial for the prevention and treatment of AP. It is crucial to elucidate the mechanisms that trigger and regulate resistance to pancreatic acinar cell death. JOSD2 expression was significantly upregulated in the pancreas of CER-induced mouse AP models. In vivo studies showed that JOSD2 deficiency attenuated CER- or L-arginine-induced pancreatic injury and inflammation. Acinar cell JOSD2 was shown to regulate pancreatic acinar cell injury, including apoptosis and DNA lesions. PCNA was identified as a key substrate of JOSD2 through LC-MS/MS analysis. Mechanistically, JOSD2 directly cleaved the K63-linked poly-ubiquitin on PCNA at residue K164 via its active site C24, thereby suppressing its DNA damage repair activity. Furthermore, JOSD2 KO significantly reduced CER-induced DNA lesions and acinar cell death. Collectively, JOSD2 represents a promising therapeutic target for AP through the inhibition of acinar cell death.

Acinar cell death, including apoptosis and necrosis, is a well-established central initiator and promoter of AP. Cell fate, whether survival or death, is tightly regulated, and proteins are involved in all aspects of cellular function; thus, maintaining their quality and homeostasis is essential for cell survival and function.[43,44] Ubiquitination is one of the most common PTMs that regulate protein function and stability.[13,45] Furthermore, ubiquitination plays a critical role in regulating pathological DNA damage and cell death.[46–48] For instance, Traf6 in acinar cells serves as a protective factor in acute edematous pancreatitis by suppressing apoptosis, whereas LPS-induced Socs1 and Socs3 directly bind with Traf6, promoting its ubiquitin-dependent degradation, which exacerbates the progression from mild to severe AP.[49] Additionally, the E3 ubiquitin ligase, MARCH9, suppresses the progression of AP by promoting the ubiquitination and proteasomal degradation of NADPH oxidase-2 in acinar cells, thereby inhibiting reactive oxygen species (ROS) generation and NLRP3-mediated pyroptosis.[50] Our findings demonstrate that JOSD2 regulates pancreatic injury by deubiquitinating PCNA and preventing its DNA damage repair activity.

In the early phase of AP, injured acinar cells recruit immune cells to the pancreas by releasing various inflammatory mediators, including chemokines and cytokines. These immune cells are further activated by several DAMPs released from dying acinar cells, which in turn produce additional inflammatory mediators and exacerbate the condition.[51] A previous study has demonstrated that circulating genomic DNA (gDNA) is remarkably increased following single overdose injection of CER in mice.[37] Circulating histones and nucleosomes in patients with AP are related to the severity of AP, as evidenced by several prospective studies.[52,53] Although the relevance of DNA damage in disease pathogenesis remains insufficiently investigated, available results indicated that both L-arginine and CER administration could promote DNA damage, cell death and DAMPs release.[28] Increasing evidence has underscored the pivotal role of inflammation and immune cells in AP.[54,55] However, our bone marrow transplantation assays revealed that JOSD2 in myeloid cells does not contribute to AP progression, whereas acinar cell-specific JOSD2 deletion partially inhibited the release of inflammatory cytokines and DAMPs in vitro. Additionally, JOSD2 deficiency suppressed the activation of MAPKs and NF-κB signaling pathways during AP. Previous studies have shown that extrinsic stimuli can result in acinar cell inflammation, which is crucial for local and systemic inflammatory responses.[56–58]

The biological role of DUBs is determined by their specific substrates. Through LC-MS/MS analysis, PCNA was identified as a substrate of JOSD2, a finding verified by co-IP experiments in 293T cells. PCNA is a well-established cell cycle regulator and serves as a proliferation marker for cells.[59,60] Additionally, PCNA activity is regulated by various PTMs, including ubiquitination, sumoylation, acetylation, and phosphorylation.[61] Ubiquitination of PCNA at lysine residue K164 is particularly critical for regulating DNA damage tolerance (DDT).[61,62] DDT, which includes translesion synthesis (TLS) and template switching (TS), occurs as a response to DNA damage, preventing DNA double-strand breaks (DSBs) and maintaining genomic stability and cell survival.[63] Upon DNA damage, mono-ubiquitination of PCNA at K164, mediated by the Rad6-Rad18 complex, triggers TLS, whereas subsequent K63-linked polyubiquitination at the same residue by the Mms2-Ubc13-Rad5 complex promotes TS.[64,65] Several DUBs have been reported to regulate PCNA deubiquitination in DDT pathways.[66] For example, USP1 and USP7 remove mono-ubiquitin from PCNA, thereby inhibiting TLS under DNA replication stress, leading to increased mutagenesis frequency.[67,68] USP7 has also been shown to remove both K63-linked poly-ubiquitin and mono-ubiquitin from PCNA in cell-free systems.[69] Based on this, it is

Figure 5. (*See previous page*). JOSD2$^{-/-}$ mice show less severe pancreas and lung injury in the L-arginine-induced AP model. (*A*) Schematic illustration of a L-arginine-induced AP model. (*B*) Survival (Kaplan-Meier) curves (n = 16) of WT and JOSD2$^{-/-}$ mice subjected to L-arginine injection. (*C*) Gross pancreatic images 72 hours after the first injection of L-arginine. (*D*) Pancreas weight to body weight ratio in WT and JOSD2$^{-/-}$ mice after L-arginine injection. (*E–G*) Pancreatic trypsin activity, serum amylase, lipase, and LDH levels in serum obtained from L-arginine-induced WT and JOSD2$^{-/-}$ mice (n = 6). Representative H&E staining images (*H*) and corresponding quantification (*I*) of pancreas and lung sections obtained from WT and JOSD2$^{-/-}$ mice treated with L-arginine (n = 6). Scale bar: 100 μm. (*J*) Immunohistochemistry images of F4/80-stained pancreas and lung sections from WT and JOSD2$^{-/-}$ mice treated with L-arginine (n = 6). Scale bar: 100 μm. (*K*) Corresponding quantification of F4/80-stained pancreas and lung sections from WT and JOSD2$^{-/-}$ mice with L-arginine-induced AP (n = 6). (*L*) *Il6* and *Tnf* mRNA expression in the pancreas tissues from indicated groups. Data were normalized by GAPDH (n = 6). Data are presented as means ± SD; $^{**}P < .01$, $^{***}P < .001$. L-arg, L-arginine. All experimental animals were female.

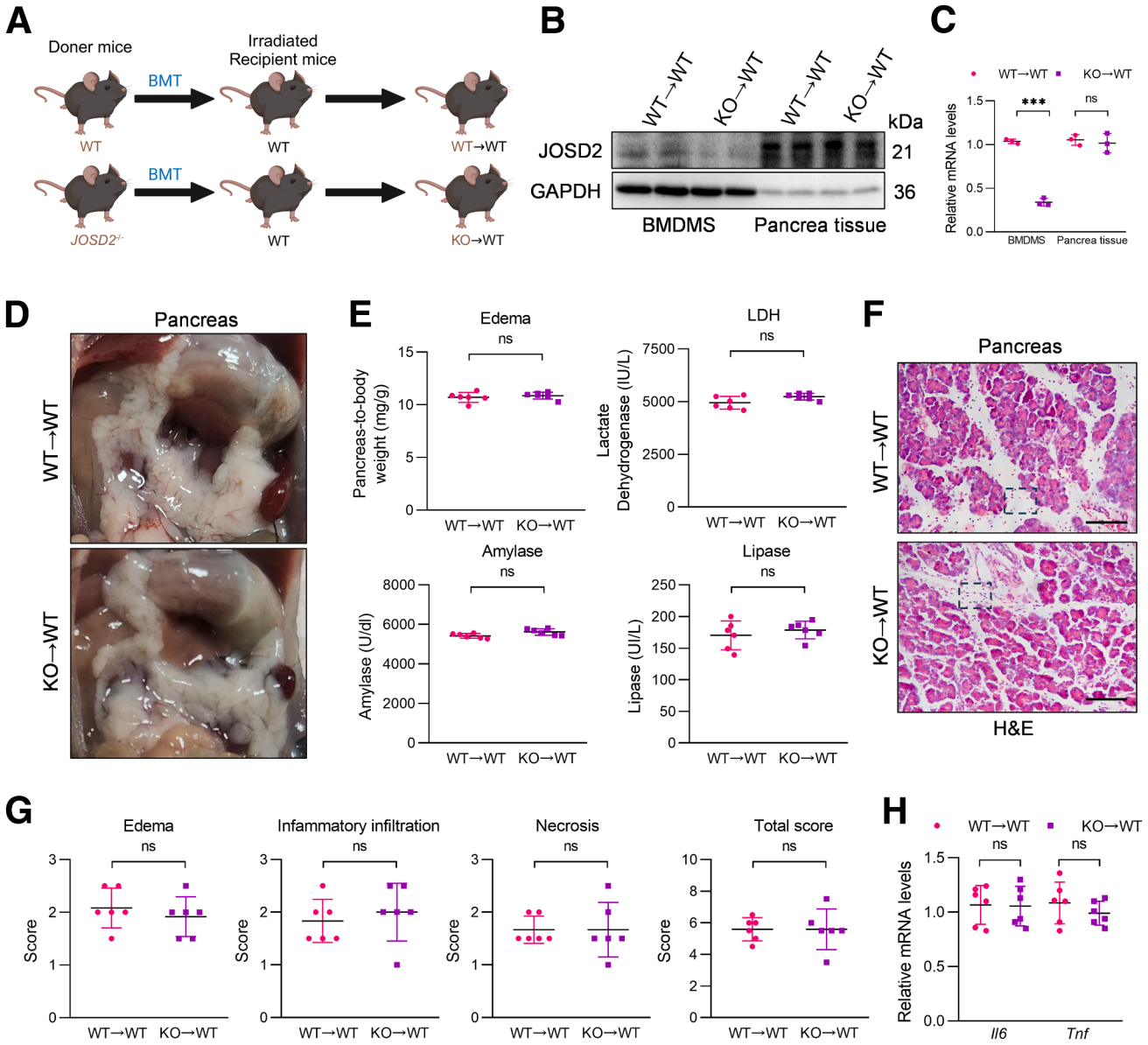

Figure 6. Myeloid cells JOSD2 did not affect pancreatic injury and inflammation response in mice with single CER cycle-induced AP. (*A*) Schematic illustration of bone marrow transplantation experiment to generate bone marrow chimeric mice. WT→WT, WT mice were irradiated and reconstituted with bone marrow from WT mice; KO→WT, WT mice were irradiated and reconstituted with bone marrow from JOSD2$^{-/-}$ mice. (*B–C*) The protein and mRNA levels of JOSD2 in BMDMs and pancreas of mice from 2 groups were examined using Western blot analysis and qPCR. (*D*) Gross pancreatic images were determined in WT→WT and KO→WT mice following 8 times CER injection (n = 6). (*E*) Ratio of pancreas weight to body weight and serum LDH, amylase, and lipase levels of WT and JOSD2$^{-/-}$ mice (n = 6). (*F*) Representative images of H&E-stained pancreas sections from WT→WT and KO→WT mice after CER stimulation (n = 6). Scale bar: 100 μm. (*G*) Histopathologic scoring of pancreas edema, inflammation infiltration and necrosis in pancreas tissues from WT→WT and KO→WT mice (n = 6). (*H*) Inflammatory cytokines *Il6* and *Tnf* mRNA expression in the pancreas tissues from indicated groups. Data were normalized against GAPDH (n = 6). All data are presented as means ± SD; ns no significant. All experimental animals were female.

hypothesized that PCNA ubiquitination might participate in DNA damage repair during acinar cell injury. This study demonstrated that DNA damage induced by CER in acinar cells can be reversed by JOSD2 deletion. Mechanistically, the loss of JOSD2 suppressed acinar cell death by maintaining K63-linked ubiquitination of PCNA, promoting DNA TS and enhancing genomic stability.

PCNA-I1, a small-molecule inhibitor of PCNA, binds to the PCNA trimer structure and subsequently reduces chromatin-associated PCNA, thereby inhibiting prostate tumor cell growth and enhancing cisplatin-induced DNA damage and apoptosis both in vitro and in vivo.[36] Although the specific effects of PCNA-I1 in acinar cells are not well-defined, the current study demonstrated that the protective effects of

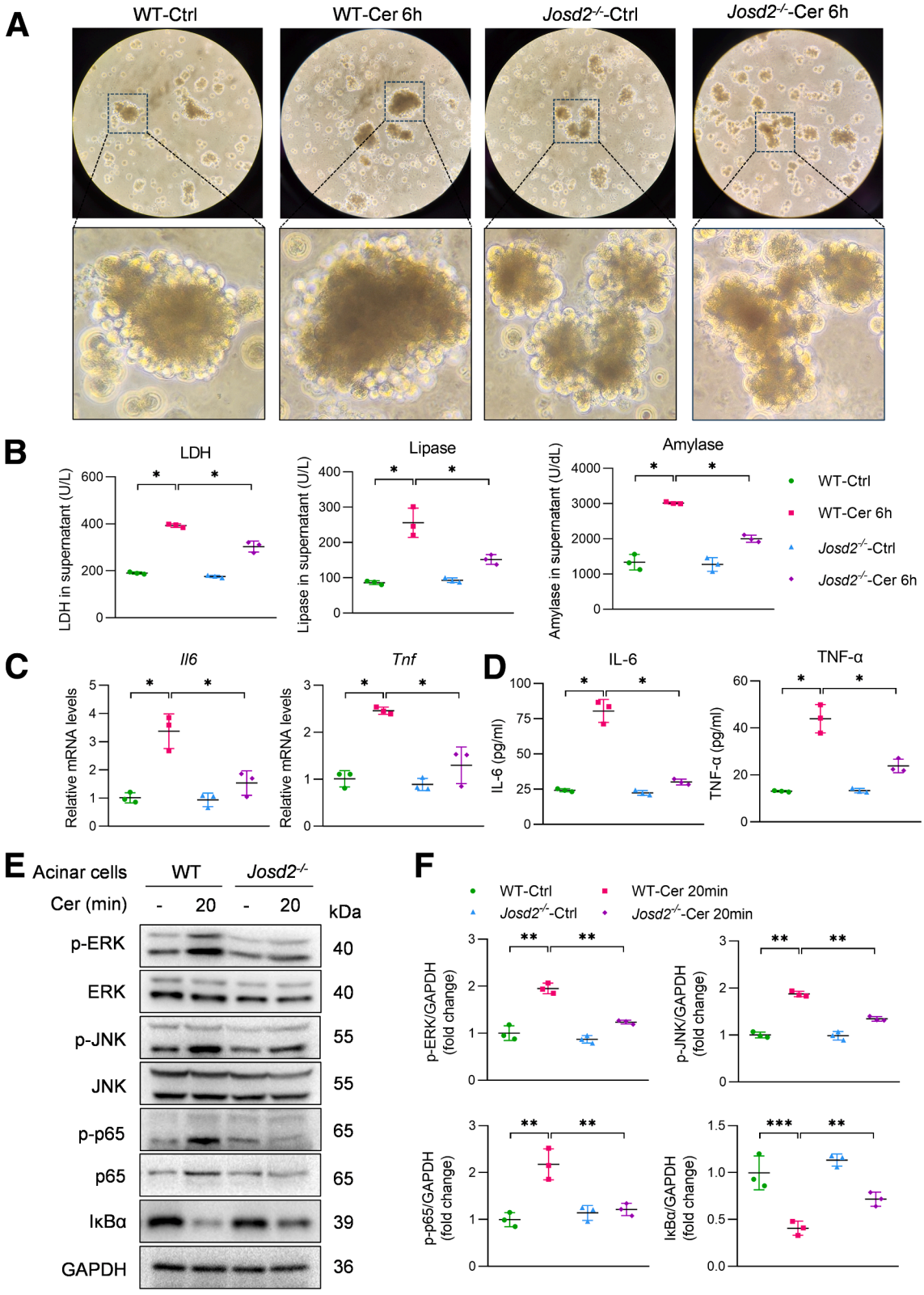

Figure 7. JOSD2$^{-/-}$ primary acinar cells represent less sensitive to CER stimulation. Acinar cell morphology images (*A*) and LDH, amylase, and lipase concentrations in the supernate of acinar cells (*B*) after CER stimulation for 6 hours (n = 3). (*C*) RT-qPCR analysis of *Il6* and *Tnf* mRNA levels in acinar cells from WT and JOSD2$^{-/-}$ mice treated with CER for 6 hours; Data of mRNA levels were normalized to GAPDH (n = 3). (*D*) ELISA analysis of IL-6 and TNF-α levels in the supernatants of acinar cell with CER treatment for 6 hours (n = 3). (*E*) Western blot analysis of the activity of MAPKs and NF-κB in acinar cells of each group. GAPDH served as the loading control (n = 3). (*F*) Densitometric quantification of Western blot image showing in panel E. Data are shown as means ± SD; **P* < .05, ***P* < .01, ****P* < .001. All experimental animals were female.

JOSD2-knockdown on DNA damage and acinar cell death were reversed by PCNA-I1 treatment. These findings suggest that JOSD2 mediates CER-induced acinar cell injury by impairing the DNA damage repair activity of PCNA.

In addition to PCNA, whether there are still other substrate proteins could mediated acute pancreatitis by JOSD2-dependent manner remains unclear. Our interaction proteomics shown that there are 11 potential substrate

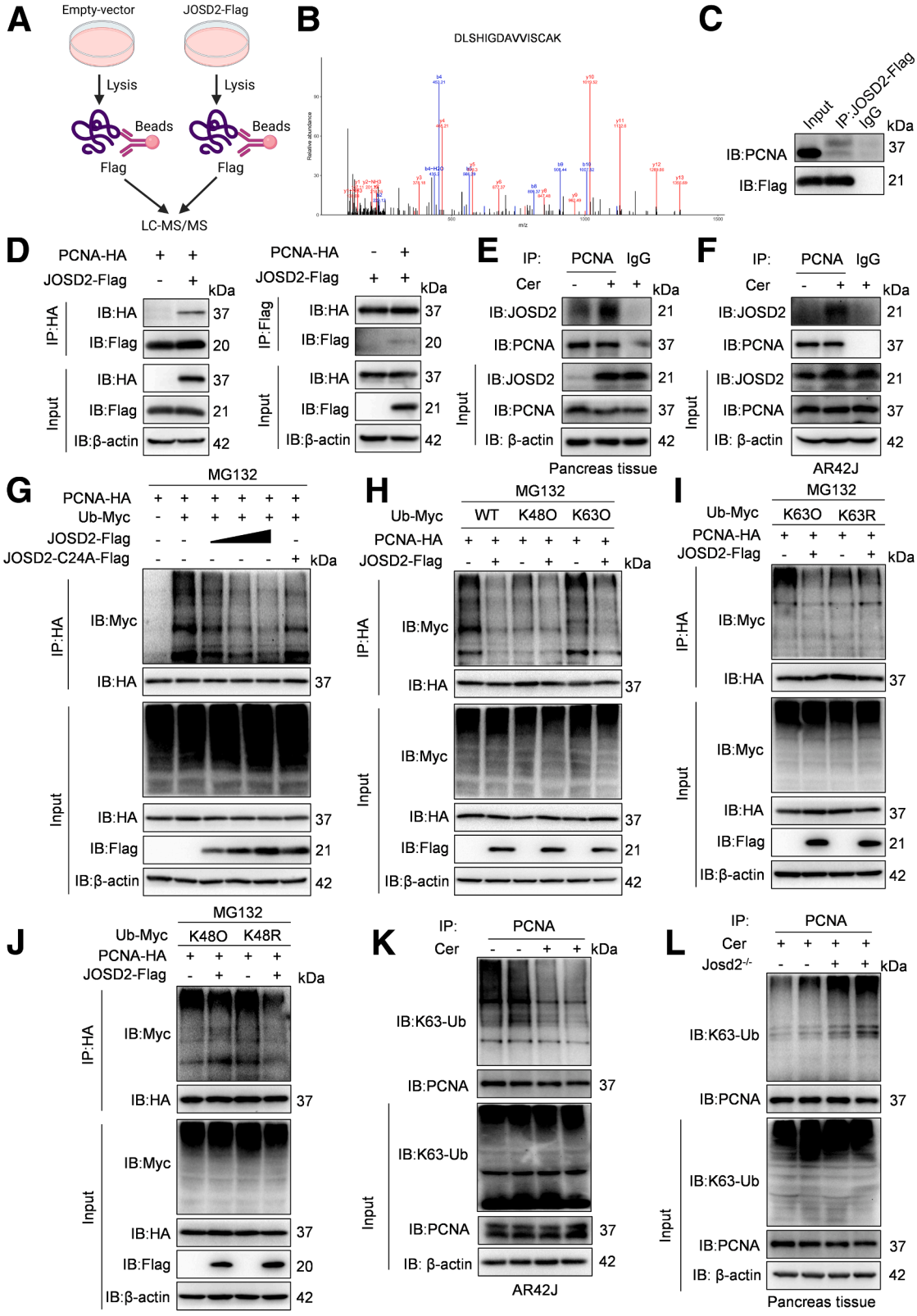

Table 1. Top 11 Potential Substrate Proteins of JOSD2

Rank	Protein name	MW, *kDa*	Coverage, %	LFQ intensity IP_Ctrl	LFQ intensity IP_JOSD2	IP_JOSD2/IP_Ctrl Ratio
1	JOSD2	20.756	93.1	423130	4836000000	11428.403
2	CBS	60.586	11.6	6989600	14986000	2.144
3	EIF6	26.599	41.2	13204000	23835000	1.805
4	IPO9	115.96	3.3	2785200	4844100	1.739
5	LMNB1	66.408	7.5	6165900	10079000	1.635
6	IMPDH2	55.804	54.1	68790000	111400000	1.619
7	DDOST	50.8	11	8006500	12807000	1.6
8	GIGYF2	150.07	6.6	9058600	14339000	1.583
9	FAM133B	28.385	18.6	124870000	196080000	1.57
10	MED26	65.446	5.5	8399600	12774000	1.521
11	PCNA	28.768	13	17911000	27102000	1.513
12	SYMPK	141.15	3.9	5784700	8743800	1.512

proteins of JOSD2 (Table 1). Among them, cysthionine-β-synthase (CBS) is a key coenzyme in glutathione (GSH) synthesis, and stabilizing or activating CBS could improve ROS-mediated pancreatical damage.[70–72] Among the numerous substrates of JOSD2 previously reported, NLRP3[73,74] and CaMKIIδ[75,76] may be involved in AP.

However, this study has limitations. The first limitation is the absence of acinar cell-specific JOSD2 KO mice to confirm the hypothesis. Secondly, it did not explore whether JOSD2 removes mono-ubiquitin from PCNA. Moreover, further research is needed to examine the role of DDT mechanisms, including TLS and TS, in acinar cells and the association of PCNA's trimer structure with DNA during AP. These areas merit further investigation to fully understand the impact of JOSD2 on acinar cell survival.

In conclusion, this study demonstrated that JOSD2 deubiquitinates K63-linked polyubiquitination at lysine residue K164 and regulates DNA damage repair in acinar cells. The findings underscore the critical role of JOSD2 in maintaining pancreatic homeostasis by mediating acinar cell death, positioning JOSD2 as a potential therapeutic target for the treatment of AP.

Materials and Methods

Mice

Mouse studies were initiated following the review and approval of care and experimental procedures by the Wenzhou Medical University Animal Policy and Welfare Committee (Approval Document No. wydw2022-0745). All animal experiments conformed to the National Institutes of Health guidelines (Guide for the Care and Use of Laboratory Animals). WT C57BL/6J mice were obtained from Gempharmatech Co, Ltd. JOSD2$^{-/-}$ mice with a C57BL/6J background were generously provided by Prof Fuping You (Peking University). JOSD2$^{-/-}$ mice were hybridized with WT mice to obtain F1 progeny, and JOSD2$^{-/-}$ mice and littermate controls were obtained through F1/F2 self-crossing. As in our previous study, both genotyping[25] and Western blot[23] analyses confirmed that JOSD2 was knocked out in JOSD2$^{-/-}$ mice in this study. All mice were housed under specific pathogen-free conditions with a 12-hour light/dark cycle at 22°C ± 2°C and 40% to 70% humidity.

Animal Experiments

For CER-induced AP, female WT, and JOSD2$^{-/-}$ mice (aged 7–8 weeks) were fasted for 12 hours before receiving intraperitoneal injections of CER at a dose of 50 μg/kg (Cat#: HY-A0190, MedChemExpress) every hour for 8 injections or 8 injections on 3 consecutive days. Control mice received saline injection at the same time points. Mice were humanely euthanized 1 hour after the final injection, and serum, pancreas, and lung samples were collected for further analysis. For L-arginine-induced AP, female WT and JOSD2$^{-/-}$ mice (aged 7–8 weeks) were fasted for 12 hours. AP was induced via 2 intraperitoneal injections of L-arginine (4 g/kg; Cat#: 1119-34-2, Sigma-Aldrich) at 1-hour intervals. Control mice received

Figure 8. (***See previous page***). **JOSD2 binds directly to PCNA and removes its ubiquitin chains at lysine 164.** (*A*) Schematic illustration of proteomics analysis to detect the substrate of JOSD2. (*B*) MS/MS spectrum showing the peptide of DLSHIGDAVVISCAK from PCNA. (*C*) Co-IP assay of JOSD2 and PCNA in 293T cells transfected with Flag-JOSD2. Anti-FLAG magnetic beads were used for immunoprecipitation. (*D*) Co-IP assay of JOSD2 and PCNA in 293T cells cotransfected with Flag-JOSD2 and HA-PCNA. Anti-FLAG magnetic beads and anti-HA magnetic beads were used for immunoprecipitation, respectively. (*E*) Co-IP of JOSD2 and PCNA in pancreas tissue treated with Cerulein. (*F*) Co-IP of JOSD2 and PCNA in CER-challenged AR42J. (*G–J*) Western blot analysis of ubiquitination levels of HA-PCNA in 293T cells cotransfected with the indicated plasmids followed by 10 μM MG132 treatment for 6 hours. Immunoprecipitation was performed with anti-HA magnetic beads. (*K*) Ubiquitinated PCNA was detected by immunoblotting using a K63-Ub antibody to clarify the K63-linked ubiquitination pattern of PCNA in AR42J treated with or without CER. (*L*) Lysates of pancreas tissue from WT and JOSD2$^{-/-}$ mice were subjected to co-IP with anti PCNA, which was followed by immunoblot with an anti-K63-Ub antibody.

the same volume of saline by intraperitoneal injection. Seventy-two hours after the first injection, the mice were euthanized following excessive anesthesia, and serum, pancreas, and lung samples were collected.

Cell Culture and Transfection

HEK-293T cells (Cat#: GNHu17) were obtained from the National Infrastructure of Cell-line Resource. The cells were cultured in Dulbecco's modified Eagle medium (DMEM)

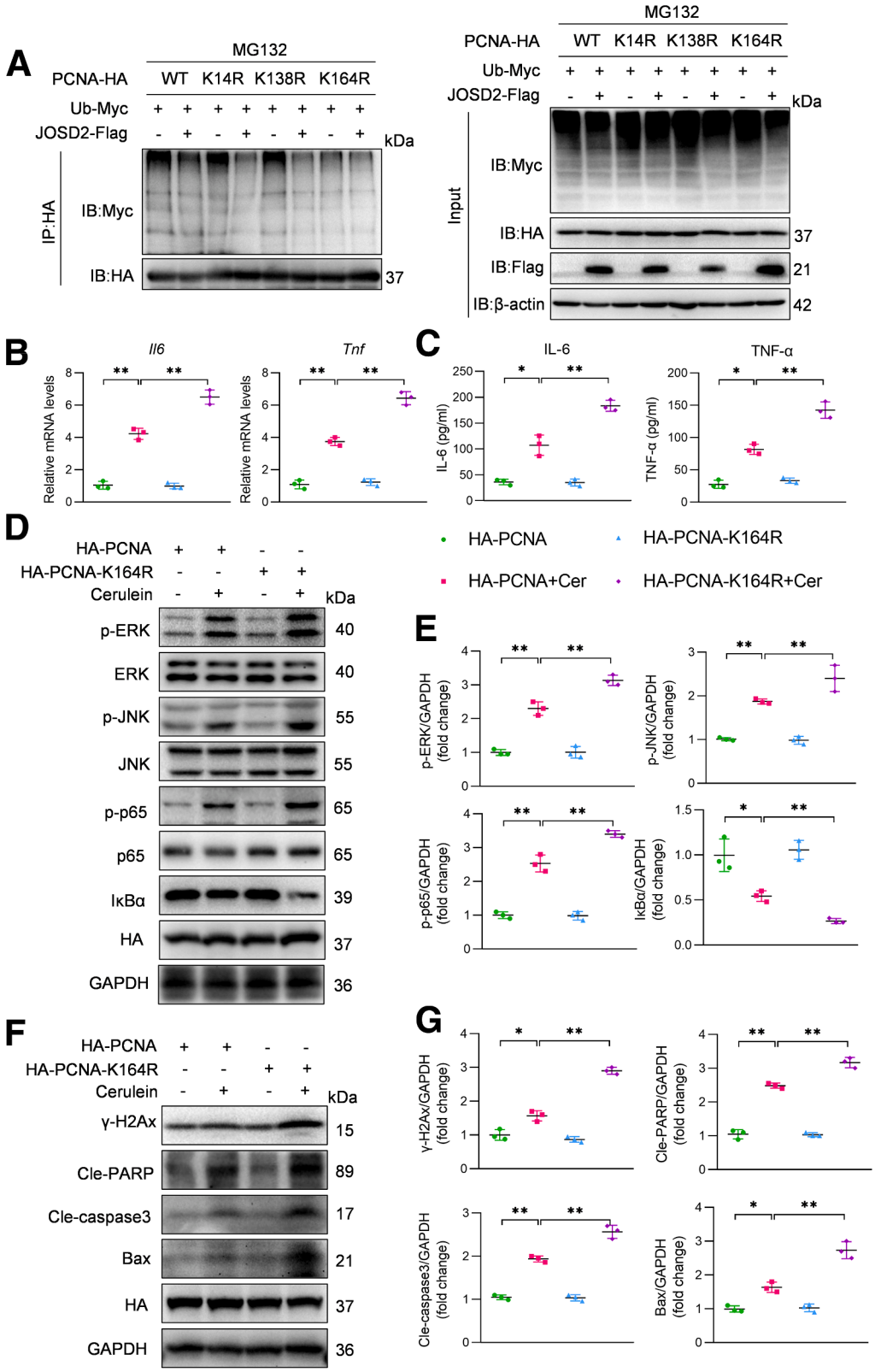

(Cat#: C11995500BT, Gibco) supplemented with 10% fetal bovine serum (FBS) (Cat#: BC-SE-FBS07, Nanjing SenBeiJia Biological Technology Co, Ltd). The plasmids JOSD2-Flag, JOSD2-C24A-Flag, PCNA-HA, HA-PCNA-K14R, HA-PCNA-K138R, and HA-PCNA-K164R were purchased from Tsingke Biotechnology, whereas Myc-Ub-WT, Myc-Ub-K48O, Myc-Ub-K63O, Myc-Ub-K48R, and Myc-Ub-K63R plasmids were acquired from keLei Biological Technology. Plasmid transfections were conducted using Lipofectamine 3000 reagent (Cat#: L3000015, Invitrogen) according to the manufacturer's protocol.

The AR42J (Rat pancreatic acinar cell line) cell (Cat#: CL-0025, Pricella Biotechnology Co, Ltd) were cultured in Ham's F-12 K medium (Cat#: PM15910, Pricella Biotechnology Co, Ltd) supplemented with 20% FBS and 1% penicillin and streptomycin in a humid incubator (37°C, 5% CO_2). For transfection, cells were seeded at 70% confluency in 60-mm tissue culture dishes. After 24 hours, cells were transiently transfected with plasmids PCNA-HA and HA-PCNA-K164R using Lipofectamine 3000 reagent (Cat#: L3000015, Invitrogen) according to the manufacturer's protocol. The cell model of AP was created by treating cells with CER (10 nM).

Biochemical Analysis

The activity levels of amylase, lipase, and LDH in serum and supernatant were measured using α-amylase assay kits (Cat#: C016-1-1, Nanjing Jiancheng), lipase assay kits (Cat#: A054-2-1, Nanjing Jiancheng), and LDH assay kits (Cat#: A020-2-2, Nanjing Jiancheng), respectively, following the manufacturer's protocols.

Enzyme-linked Immunosorbent Assay

The levels of IL-6 and TNF-α in serum and acinar cell culture supernatants were measured using IL-6 Mouse enzyme-linked immunosorbent assay (ELISA) Kits (Cat#: 88-7064-88, ThermoFisher) and TNF-α ELISA Kits (Cat#: 88-7324-76, ThermoFisher), according to the manufacturer's instructions.

MPO Activity

MPO activity was measured following previously established protocols.[77] Pancreas and lung tissues were homogenized in 100 mM phosphate buffer (pH 7.4) containing protease inhibitors (Cat#: P1051, Beyotime) and centrifuged at 16,000 × g for 15 minutes at 4°C. The pellets were washed by resuspension in phosphate buffer (pH 7.4) and centrifuged again. After washing, the pellets were resuspended in 100 mM phosphate buffer (pH 5.4) containing 0.5% hexadecyltrimethylammonium bromide (Cat#: H6269, Sigma-Aldrich), 10 mM EDTA, and protease inhibitors. The suspension underwent 3 cycles of sonication, freezing, and thawing. The extract was then centrifuged at 16,000 × g for 15 minutes at 4°C. MPO activity in the supernatants was determined using a colorimetric method with 3,3′,5,5′-trimethylbenzidine (TMB) and 0.03% H_2O_2. The supernatants were incubated with TMB for 3 minutes at 37°C, followed by the addition of 0.03% H_2O_2 and further incubation for 3 minutes. The reaction was stopped with 2N H_2SO_4. Absorbance was measured at 655 nm. Protein concentration in the supernatants was determined using the Micro BCA Protein Assay Kit (Cat#: 23235, ThermoFisher), and MPO activity was expressed as mU/mg protein.

RT-qPCR

Total RNA was extracted from mouse pancreas tissues and acinar cells using RNAiso Plus (Cat#: 9109, TAKARA). The extracted RNA was reverse-transcribed into complementary DNA using the TransScript All-in-One First-Strand cDNA Synthesis SuperMix (Cat#: AT341, TransGen Biotech). Quantitative PCR was conducted using PerfectStart Green qPCR SuperMix (Cat#: AQ601, TransGen Biotech) in a QuantStudio 3 real-time PCR system (ThermoFisher). The PCR conditions were as follows: initial denaturation at 95°C for 1 minute, followed by 45 cycles of 95°C for 10 seconds, 60°C for 30 seconds, and 72°C for 30 seconds.

The primers used in this study were listed as follows: *Il6* (Mouse), 5′-GAGGATACCACTCCCAACAGACC-3′ (forward), and 5′-AAGTGCATCATCGTTGTTCATACA-3′ (reverse); *Tnf* (Mouse), 5′-CTGAGGTCAATCTGCCCAAGTAC-3′ (forward), and 5′-CTTCACAGAGCAATGACTCCAAAG-3′ (reverse); *JOSD2* (Mouse), 5′-CTGATCTTGAACCTACCCTCTC-3′ (forward), and 5′-CGGAGCTTTGAGTCCAGATTAT-3′ (reverse); *GAPDH* (Mouse), 5′-TGTGTCCGTCGTGGATCTGA-3′ (forward), and 5′-CCTGCTTCACCACCTTCTTGA-3′ (reverse).

Histological Analysis

Pancreas and lung tissues were fixed in 4% paraformaldehyde and embedded in paraffin. Sections of pancreas and lung tissue (5 μm) were stained with H&E (Cat#: G1120, SolaR-bio Life Science) for histopathological assessment. The severity of the pancreatic injury was

Figure 9. (***See previous page***). **JOSD2 knockout attenuates AP via PCNA activity.** (*A*) Schematic illustration showing in vitro experiments conducted to identify whether PCNA is necessary for JOSD2-mediated progression of AP. (*B*) LDH, amylase, and lipase levels in the supernate of acinar cells from WT and JOSD2$^{-/-}$ mice primed with PCNA-I1 and followed by CER stimulation (n = 3). RT-qPCR analysis of *Il6* and *Tnf* mRNA levels (*C*) in acinar cells and ELISA analysis of IL-6 and TNF-α concentrations in supernatant (*D*) were performed. Data of mRNA levels were normalized to GAPDH (n = 3). (*E*) Western blot analysis of the activity of MAPKs and NF-κB in acinar cells from WT and JOSD2$^{-/-}$ mice pretreated with PCNA-I1 and subjected to CER. (*F*) Densitometric quantification of Western blot image shown in panel *E*. (*G*) Western blot analysis of the levels of DNA damage marker (γ-H2Ax and Cle-PARP) and pro-apoptotic protein (Cle-caspase 3 and Bax) in acinar cells from WT and JOSD2$^{-/-}$ mice pretreated with PCNA-I1 and subjected to CER. GAPDH served as the loading control (n = 3). (*H*) Densitometric quantification of Western blot image shown in panel *G*. Data are shown as means ± SD; *$P < .05$. All experimental animals were female.

evaluated using the following scoring criteria as described previously:[78] edema score (0–3; 0 = absent, 1 = focally increased between lobules, 2 = diffusely increased, 3 = acini disrupted and separated), inflammatory infiltration score (0–3; 0 = absent, 1 = around the pancreatic duct, 2 = intralobular or perivascular infiltration <50% of the lobules, 3 = intralobular or perivascular infiltration >50% of the lobules), necrosis score (0–3; 0 = absent, 1 = periductal

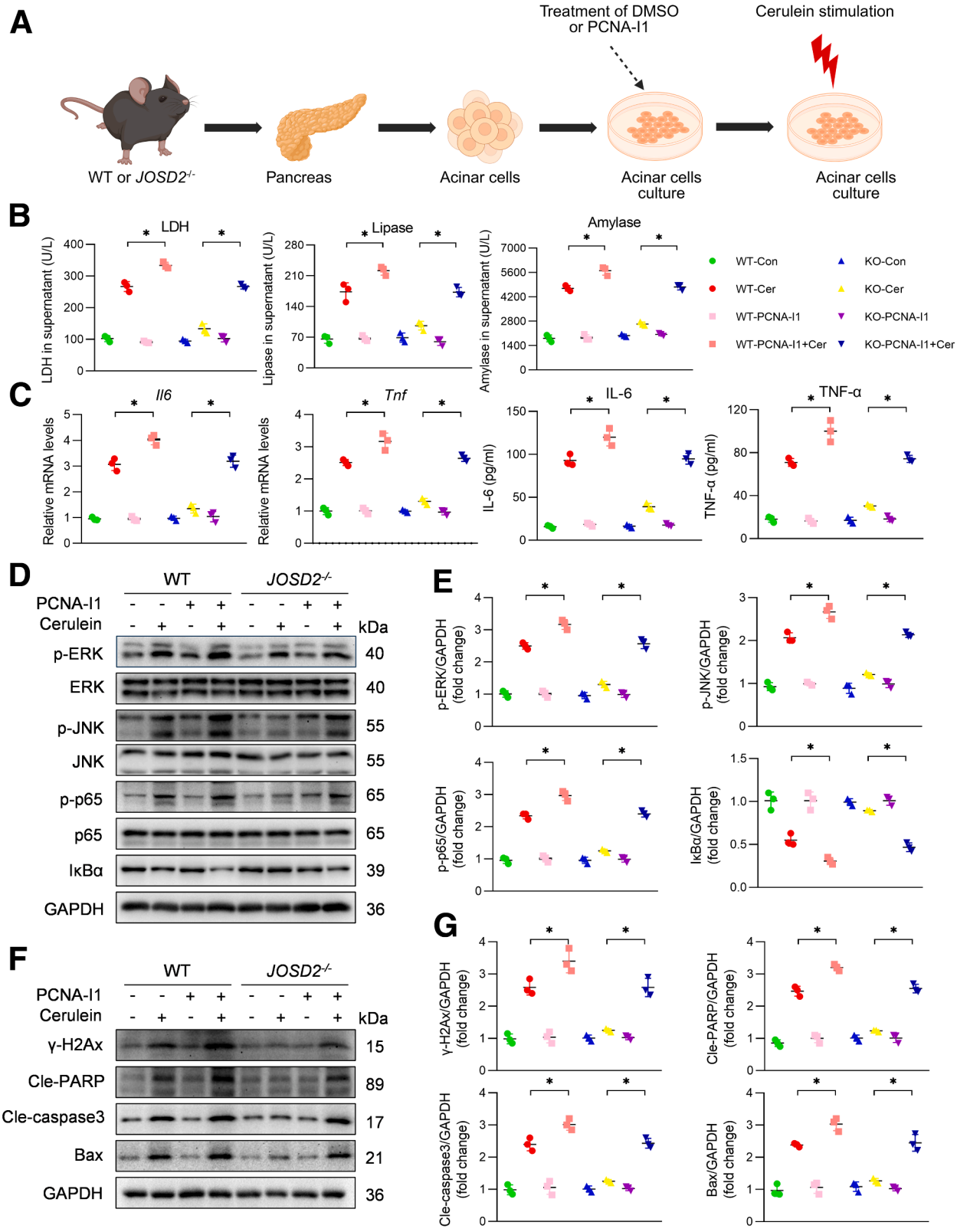

necrosis, <5% cells, 2 = focal necrosis, 5%–20% cells, 3 = diffuse parenchymal necrosis, 20%–50% cells), and a total score (sum of edema, inflammatory infiltration, and necrosis scores).

Immunohistochemistry Staining

Paraffin sections (5-μm thick) were dewaxed, rehydrated, and subjected to antigen retrieval in 100 mM citrate buffer (pH 6.0) at 120°C for 3 minutes. The sections were incubated with 3% H_2O_2 for 10 minutes to block endogenous peroxidase activity. Nonspecific binding was blocked by incubating the sections with 10% normal goat serum (Cat#: SL038, Solarbio) for 30 minutes. Primary antibodies against F4/80 (Cat#: 70076, Cell Signaling Technology) and MPO (Cat#: 390109, Santa Cruz Biotechnology) were applied at room temperature for 2 hours, followed by incubation with horseradish peroxidase (HRP)-linked secondary antibodies (Cat#: A0216, Beyotime Biotechnology). The immune signal intensity was detected using a DAB kit (Cat#: ZLI-9018, Zhong Shan-Golden Bridge Biological Technology Co, Ltd). Immunohistochemical images were captured using a light microscope (Nikon).

Western Blot Analysis

Cells and pancreatic tissues were lysed using RIPA buffer (Cat#: P0013B, Beyotime Biotechnology) containing a protease and phosphatase inhibitor cocktail (Cat#: P1051, Beyotime). Protein concentrations were quantified using a Bradford protein assay kit (Cat#: 5000205, Bio-Rad). Equal amounts of protein sample were separated by 10% to 12% sodium dodecyl sulfate-polyacrylamide gel electrophoresis (SDS-PAGE) and transferred to polyvinylidene difluoride (PVDF) membranes (BioRad). The membranes were blocked with 5% skim milk in 0.1% TBST for 1 hour at room temperature to prevent nonspecific binding, followed by incubation with primary antibodies overnight at 4°C. After washing with 0.1% TBST for 3 5-minute intervals, the membranes were incubated with corresponding secondary antibodies for 1 hour at room temperature. Protein signals were enhanced using ECL detection reagents (Cat#: P10300, NCM Biotech) and visualized using the ChemiDoc XRS+ system (Bio-Rad). Quantification of protein bands was performed using ImageJ software. Primary antibodies against MYC (Cat#: 2276), p-NF-κB p65 (Cat#: 3033), NF-κB p65 (Cat#: 8242), IκBα (Cat#: 4812), p-JNK (Cat#:4668), JNK (Cat#:9252), p-ERK (Cat#:4370), ERK (Cat#:4695), glyceraldehyde-3-phosphate dehydrogenase (GAPDH) (Cat#: 5174), Cle-caspase3 (Cat#:9664), BAX (Cat#:14796), Cle-PARP (Cat#:9544), γ-H2AX (Cat#:2577) were purchased from Cell Signaling Technology. Antibodies against HA (Cat#: 51064-2-AP), Flag (Cat#: 66008-4-Ig), β-actin (Cat#: 66009-1- Ig), PCNA (Cat#: 60097-1- Ig) were purchased from Proteinthch. Antibodies against JOSD2 (Cat#: orb184482) was purchased from Biorbyt. And the HRP-linked secondary antibodies (anti-mouse IgG, A0216; anti-rabbit IgG, A0208) were purchased from Beyotime Biotechnology.

Co-immunoprecipitation

HEK-293T cells transfected with the appropriate plasmids for 24 hours were collected and lysed using ice-cold NP-40 Lysis Buffer (50 mM Tris-HCl, pH 7.4, 150 mM NaCl, 1% NP-40) containing protease and phosphatase inhibitors cocktail (Cat#: P1051, Beyotime). The lysates were sonicated for 1 minute and centrifuged at 12,000 × g for 15 minutes at 4°C. The supernatant was incubated with target-specific antibodies overnight at 4°C, followed by a 3-hour incubation with protein A+G agarose beads (Cat#: P2055, Beyotime Biotechnology) at 4°C. The beads were washed 5 times with ice-cold lysis buffer and then eluted by boiling in loading buffer at 95°C, followed by immunoblot analysis.

Bone Marrow Transplantation

Recipient WT mice were subjected to total body irradiation (6 Gy) to deplete autologous bone marrow cells. Within 6 to 12 hours post-irradiation, 5.0×10^6 fresh bone marrow cells from donor WT or JOSD2$^{-/-}$ (KO) mice were injected intravenously into the irradiated WT mice. Eight weeks later, the WT→WT and KO→WT mice were subjected to CER-induced AP. Bone marrow-derived macrophages (BMDMs) and pancreatic tissues were collected to confirm the efficacy of the bone marrow transplantation.

Acinar Cell Preparation

Pancreatic acinar cells were isolated from WT and JOSD2$^{-/-}$ mice using collagenase digestion method as described previously.[17] Briefly, mice were humanely euthanized, and the pancreatic tissue was collected. Visible blood vessels, lymph nodes, and fat were carefully removed from the pancreas and washed with ice-cold phosphate

Figure 10. (***See previous page***). **JOSD2 deubiquitinates PCNA at K164 to block DNA damage repair in acinar cells.** (*A*) Western blot analysis of ubiquitination levels of HA-PCNA in 293T cells cotransfected with the indicated plasmids followed by 10 μM MG132 treatment for 6 hours. Immunoprecipitation was performed with anti-HA magnetic beads. (*B*) AR42J cells were transfected with HA-PCNA or HA-PCNA-K164R expressing plasmid. Cells then were treated with CER, and mRNA levels of *Il6* and *Tnf* were measured (n = 3). (*C*) IL-6 and TNF-α levels in supernatants from AR42J cells transfected with HA-PCNA or HA-PCNA-K164R expressing plasmid. Cells then were treated with CER (n = 3). (*D*) AR42J cells were transfected with HA-PCNA or HA-PCNA-K164R expressing plasmid. Then were treated with CER. Lysates then were probed for activation of downstream NF-κB pathway and MAPKs pathway proteins (n = 3). (*E*) Densitometric quantification of Western blot image shown in panel *D*. (*F*) AR42J cells were transfected with HA-PCNA or HA-PCNA-K164R expressing plasmid, then were treated with CER. Lysates then were probed for activation of DNA damage marker (γ-H2Ax and Cle-PARP) and pro-apoptotic protein (Cle-caspase 3 and Bax) (n = 3). (G) Densitometric quantification of Western blot image shown in panel *F*. Total proteins and GAPDH were used as control. Data are shown as means ± SD; ns no significant, $^*P < .05$, $^{**}P < .01$.

buffered saline (PBS). The tissue was cut into smaller pieces (approximately 1–2 mm^3) and digested in digestion solution (DMEM containing 2.5 mg/mL bovine serum albumin [BSA] [Cat#: A1933, Sigma-Aldrich], 1 mg/mL Collagenase IV [Cat#: LS004188, Worthington], and 100 μg/mL soybean trypsin inhibitor [SBTI, Cat#: LS003571, Worthington]) for 20 minutes at 37°C on a magnetic stirrer set to 180 rpm. The supernatant was discarded, and a fresh digestion solution was added to ensure complete digestion. The cell suspension was then filtered through a 100-μm nylon mesh into a rinse solution (DMEM supplemented with 10 mg/mL BSA and 100 μg/mL SBTI). Cell pellets were washed with centrifugation solution (DMEM supplemented with 40 mg/mL BSA and 100 μg/mL SBTI) and centrifuged at 50 $\times$ g for 2 minutes. This process was repeated 3 times. After the final wash, the cells were resuspended in incubation solution (DMEM supplemented with 1 mg/mL BSA and 100 μg/mL SBTI) and seeded into 6-well plates. To investigate the relationship between JOSD2 and PCNA, the PCNA inhibitor PCNA-I1 (Cat#: 444930-42-1, TargetMol) was added to the acinar cell medium before CER treatment. Cells were then harvested for Western blot and RT-qPCR, while the supernatant was collected for ELISA analysis.

Pancreatic Trypsin Activity Assay

Trypsin activity was measured in homogenates of pancreas tissue by a fluorimetric assay as we described previously.[79] Briefly, pancreatic tissue was homogenized in ice-cold buffer containing 5 mmol/L 4-morpholineethanesulfonic acid (pH 6.5), 1 mmol/L MgSO4, and 250 mmol/L sucrose. Then, assay buffer containing 50 mmol/L Tris-HCl (pH = 8.0), 150 mmol/L NaCl, 1 mmol/L CaCl2, and 0.1 mg/mL BSA was added to the samples. Trypsin activity was measured using a specific substrate, Boc-GIn-Ala-Arg-MCA (Cat#: 4017019; Bachem), which is converted to a fluorescent product with trypsin. The mixture emits fluorescence at 440 nm with excitation at 380 nm. Purified trypsin (Cat#: 9002-07-7; Worthington) was used to generate a standard curve.

Statistical Analysis

All data are reported as means ± standard deviation (SD) in this study. Statistical significance was determined using GraphPad Prism v8.0 software. Student's *t*-test was used to analyze the differences between 2 groups, and 1-way analysis of variance (ANOVA) was applied to determine the differences among multiple groups. For the mouse survival study, Kaplan-Meier survival curves were established, followed by a log-rank test. $P < .05$ was considered significant.

References

1. Petrov MS, Yadav D. Global epidemiology and holistic prevention of pancreatitis. Nat Rev Gastroenterol Hepatol 2019;16:175–184.
2. Gaisano HY, Gorelick FS. New insights into the mechanisms of pancreatitis. Gastroenterology 2009; 136:2040–2044.
3. Yadav D, Lowenfels AB. The epidemiology of pancreatitis and pancreatic cancer. Gastroenterology 2013; 144:1252–1261.
4. Garg PK, Singh VP. Organ failure due to systemic injury in acute pancreatitis. Gastroenterology 2019; 156:2008–2023.
5. Hu Q, Yao J, Wu X, et al. Emodin attenuates severe acute pancreatitis-associated acute lung injury by suppressing pancreatic exosome-mediated alveolar macrophage activation. Acta Pharm Sin B 2022; 12:3986–4003.
6. Ahmed Ali U, Issa Y, Hagenaars JC, et al; Dutch Pancreatitis Study Group. Risk of recurrent pancreatitis and progression to chronic pancreatitis after a first episode of acute pancreatitis. Clin Gastroenterol Hepatol 2016;14:738–746.
7. Logsdon CD, Ji B. The role of protein synthesis and digestive enzymes in acinar cell injury. Nat Rev Gastroenterol Hepatol 2013;10:362–370.
8. Habtezion A, Gukovskaya AS, Pandol SJ. Acute pancreatitis: a multifaceted set of organelle and cellular interactions. Gastroenterology 2019;156:1941–1950.
9. Saluja A, Dudeja V, Dawra R, Sah RP. Early intra-acinar events in pathogenesis of pancreatitis. Gastroenterology 2019;156:1979–1993.
10. Liu K, Liu J, Zou B, et al. Trypsin-mediated sensitization to ferroptosis increases the severity of pancreatitis in mice. Cell Mol Gastroenterol Hepatol 2022;13:483–500.
11. Zhao Q, Wei Y, Pandol SJ, et al. STING signaling promotes inflammation in experimental acute pancreatitis. Gastroenterology 2018;154:1822–1835.e2.
12. Jakkampudi A, Jangala R, Reddy R, et al. Acinar injury and early cytokine response in human acute biliary pancreatitis. Sci Rep 2017;7:15276.
13. Popovic D, Vucic D, Dikic I. Ubiquitination in disease pathogenesis and treatment. Nat Med 2014;20:1242–1253.
14. Cockram PE, Kist M, Prakash S, et al. Ubiquitination in the regulation of inflammatory cell death and cancer. Cell Death Differ 2021;28:591–605.
15. Sun T, Liu Z, Yang Q. The role of ubiquitination and deubiquitination in cancer metabolism. Mol Cancer 2020;19:146.
16. Wang Y, Song M, Zhou P, et al. TNFAIP3-upregulated RIP3 exacerbates acute pancreatitis via activating NLRP3 inflammasome. Int Immunopharmacol 2021;100:108067.
17. Liu X, Luo W, Chen J, et al. USP25 deficiency exacerbates acute pancreatitis via up-regulating TBK1-NF-κB signaling in macrophages. Cell Mol Gastroenterol Hepatol 2022;14:1103–1122.
18. Liu Z, Qi M, Tian S, et al. Ubiquitin-specific protease 25 aggravates acute pancreatitis and acute pancreatitis-related multiple organ injury by destroying tight junctions through activation of the STAT3 pathway. Front Cell Dev Biol 2021;9:806850.
19. Zeng C, Zhao C, Ge F, et al. Machado-Joseph deubiquitinases: from cellular functions to potential therapy targets. Front Pharmacol 2020;11:1311.
20. Hutchins AP, Liu S, Diez D, Miranda-Saavedra D. The repertoires of ubiquitinating and deubiquitinating enzymes in eukaryotic genomes. Mol Biol Evol 2013;30:1172–1187.

21. Qian M, Yan F, Wang W, et al. Deubiquitinase JOSD2 stabilizes YAP/TAZ to promote cholangiocarcinoma progression. Acta Pharm Sin B 2021;11:4008–4019.
22. Krassikova L, Zhang B, Nagarajan D, et al. The deubiquitinase JOSD2 is a positive regulator of glucose metabolism. Cell Death Differ 2021;28:1091–1109.
23. Shen SR, Huang ZQ, Yang YD, et al. JOSD2 inhibits angiotensin II-induced vascular remodeling by deubiquitinating and stabilizing SMAD7. Acta Pharmacol Sin 2025;46:1275–1288.
24. Han J, Fang Z, Han B, et al. Deubiquitinase JOSD2 improves calcium handling and attenuates cardiac hypertrophy and dysfunction by stabilizing SERCA2a in cardiomyocytes. Nat Cardiovasc Res 2023;2:764–777.
25. Xu J, Liang S, Wang Q, et al. JOSD2 mediates isoprenaline-induced heart failure by deubiquitinating CaMKIIδ in cardiomyocytes. Cell Mol Life Sci 2024;81:18.
26. Liu X, Fang Y, Huang M, et al. Deubiquitinase JOSD2 alleviates colitis by inhibiting inflammation via deubiquitination of IMPDH2 in macrophages. Acta Pharm Sin B 2025;15:1039–1055.
27. Ying Z, Qing-Qing Z, Shi-Jie F, et al. JOSD2 alleviates acute kidney injury through deubiquitinating SIRT7 and negativity regulating SIRT7-NF-κB inflammatory pathway in renal tubular epithelial cells. Acta Pharmacol Sin 2025;46:2468–2481.
28. Kang R, Zhang Q, Hou W, et al. Intracellular Hmgb1 inhibits inflammatory nucleosome release and limits acute pancreatitis in mice. Gastroenterology 2014;146:1097–1107.
29. Yu JH, Kim H. Oxidative stress and inflammatory signaling in cerulein pancreatitis. World J Gastroenterol 2014;20:17324–17329.
30. Wang M, Lei R. Organ dysfunction in the course of severe acute pancreatitis. Pancreas 2016;45:e5–e7.
31. Liu S, Szatmary P, Lin JW, et al. Circulating monocytes in acute pancreatitis. Front Immunol 2022;13:1062849.
32. Peng C, Li Z, Yu X. The role of pancreatic infiltrating innate immune cells in acute pancreatitis. Int J Med Sci 2021;18:534–545.
33. Moldovan GL, Pfander B, Jentsch S. PCNA, the maestro of the replication fork. Cell 2007;129:665–679.
34. Andersen PL, Xu F, Xiao W. Eukaryotic DNA damage tolerance and translesion synthesis through covalent modifications of PCNA. Cell Res 2008;18:162–173.
35. Grasty KC, Weeks SD, Loll PJ. Structural insights into the activity and regulation of human Josephin-2. J Struct Biol X 2019;3:100011.
36. Dillehay KL, Lu S, Dong Z. Antitumor effects of a novel small molecule targeting PCNA chromatin association in prostate cancer. Mol Cancer Ther 2014;13:2817–2826.
37. Hoque R, Sohail M, Malik A, et al. TLR9 and the NLRP3 inflammasome link acinar cell death with inflammation in acute pancreatitis. Gastroenterology 2011;141:358–369.
38. van Dijk SM, Hallensleben NDL, van Santvoort HC, et al; Dutch Pancreatitis Study Group. Acute pancreatitis: recent advances through randomised trials. Gut 2017;66:2024–2032.
39. Matta B, Gougol A, Gao X, et al. Worldwide variations in demographics, management, and outcomes of acute pancreatitis. Clin Gastroenterol Hepatol 2020;18:1567–1575.e2.
40. Szatmary P, Grammatikopoulos T, Cai W, et al. Acute pancreatitis: diagnosis and treatment. Drugs 2022;82:1251–1276.
41. Kang R, Lotze MT, Zeh HJ, et al. Cell death and DAMPs in acute pancreatitis. Mol Med 2014;20:466–477.
42. Lee PJ, Papachristou GI. New insights into acute pancreatitis. Nat Rev Gastroenterol Hepatol 2019;16:479–496.
43. Freeman M. Feedback control of intercellular signalling in development. Nature 2000;408:313–319.
44. Sin O, Nollen EA. Regulation of protein homeostasis in neurodegenerative diseases: the role of coding and non-coding genes. Cell Mol Life Sci 2015;72:4027–4047.
45. Swatek KN, Komander D. Ubiquitin modifications. Cell Res 2016;26:399–422.
46. Vucic D, Dixit VM, Wertz IE. Ubiquitylation in apoptosis: a post-translational modification at the edge of life and death. Nat Rev Mol Cell Biol 2011;12:439–452.
47. Jesenberger V, Jentsch S. Deadly encounter: ubiquitin meets apoptosis. Nat Rev Mol Cell Biol 2002;3:112–121.
48. Jackson SP, Durocher D. Regulation of DNA damage responses by ubiquitin and SUMO. Mol Cell 2013;49:795–807.
49. Zhou X, Liu Z, Cheng X, et al. Socs1 and Socs3 degrades Traf6 via polyubiquitination in LPS-induced acute necrotizing pancreatitis. Cell Death Dis 2015;6:e2012.
50. Lin M, Jin Y, Wang F, et al. MARCH9 mediates NOX2 ubiquitination to alleviate NLRP3 inflammasome-dependent pancreatic cell pyroptosis in acute pancreatitis. Pancreas 2023;52:e62–e69.
51. Gukovsky I, Li N, Todoric J, et al. Inflammation, autophagy, and obesity: common features in the pathogenesis of pancreatitis and pancreatic cancer. Gastroenterology 2013;144:1199–1209.e4.
52. Liu T, Huang W, Szatmary P, et al. Accuracy of circulating histones in predicting persistent organ failure and mortality in patients with acute pancreatitis. Br J Surg 2017;104:1215–1225.
53. Penttilä AK, Rouhiainen A, Kylänpää L, et al. Circulating nucleosomes as predictive markers of severe acute pancreatitis. J Intensive Care 2016;4:14.
54. Habtezion A. Inflammation in acute and chronic pancreatitis. Curr Opin Gastroenterol 2015;31:395–399.
55. Xue J, Sharma V, Habtezion A. Immune cells and immune-based therapy in pancreatitis. Immunol Res 2014;58:378–386.
56. Wang Y, Wang G, Cui L, et al. Angiotensin 1-7 ameliorates caerulein-induced inflammation in pancreatic acinar cells by downregulating Toll-like receptor 4/nuclear factor-κB expression. Mol Med Rep 2018;17:3511–3518.
57. Leung PS, Ip SP. Pancreatic acinar cell: its role in acute pancreatitis. Int J Biochem Cell Biol 2006;38:1024–1030.
58. Kim H. Cerulein pancreatitis: oxidative stress, inflammation, and apoptosis. Gut Liver 2008;2:74–80.

59. Strzalka W, Ziemienowicz A. Proliferating cell nuclear antigen (PCNA): a key factor in DNA replication and cell cycle regulation. Ann Bot 2011;107:1127–1140.
60. Dietrich DR. Toxicological and pathological applications of proliferating cell nuclear antigen (PCNA), a novel endogenous marker for cell proliferation. Crit Rev Toxicol 1993;23:77–109.
61. Zhang S, Zhou T, Wang Z, et al. Post-translational modifications of PCNA in control of DNA synthesis and DNA damage tolerance-the implications in carcinogenesis. Int J Biol Sci 2021;17:4047–4059.
62. Che J, Hong X, Rao H. PCNA ubiquitylation: instructive or permissive to DNA damage tolerance pathways? Biomolecules 2021;11:1543.
63. Branzei D, Psakhye I. DNA damage tolerance. Curr Opin Cell Biol 2016;40:137–144.
64. Bellí G, Colomina N, Castells-Roca L, Lorite NP. Post-translational modifications of PCNA: guiding for the best DNA damage tolerance choice. J Fungi (Basel) 2022;8:621.
65. Mailand N, Gibbs-Seymour I, Bekker-Jensen S. Regulation of PCNA-protein interactions for genome stability. Nat Rev Mol Cell Biol 2013;14:269–282.
66. Masuda Y, Masutani C. Spatiotemporal regulation of PCNA ubiquitination in damage tolerance pathways. Crit Rev Biochem Mol Biol 2019;54:418–442.
67. Huang TT, Nijman SM, Mirchandani KD, et al. Regulation of monoubiquitinated PCNA by DUB autocleavage. Nat Cell Biol 2006;8:339–347.
68. Kashiwaba S, Kanao R, Masuda Y, et al. USP7 is a suppressor of PCNA ubiquitination and oxidative-stress-induced mutagenesis in human cells. Cell Rep 2015;13:2072–2080.
69. Masuda Y, Kanao R, Kawai H, et al. Preferential digestion of PCNA-ubiquitin and p53-ubiquitin linkages by USP7 to remove polyubiquitin chains from substrates. J Biol Chem 2019;294:4177–4187.
70. Sidhapuriwala JN, Hegde A, Ang AD, et al. Effects of S-propargyl-cysteine (SPRC) in caerulein-induced acute pancreatitis in mice. PLoS One 2012;7:e32574.
71. Tamizhselvi R, Moore PK, Bhatia M. Hydrogen sulfide acts as a mediator of inflammation in acute pancreatitis: in vitro studies using isolated mouse pancreatic acinar cells. J Cell Mol Med 2007;11:315–326.
72. Rius-Pérez S, Pérez S, Torres-Cuevas I, et al. Blockade of the trans-sulfuration pathway in acute pancreatitis due to nitration of cystathionine β-synthase. Redox Biol 2020;28:101324.
73. Papantoniou K, Aggeletopoulou I, Michailides C, et al. Understanding the role of NLRP3 inflammasome in acute pancreatitis. Biology (Basel) 2024;13:945.
74. Ferrero-Andres A, Panisello-Rosello A, Rosello-Catafau J, Folch-Puy E. NLRP3 inflammasome-mediated inflammation in acute pancreatitis. Int J Mol Sci 2020;21:5386.
75. Zhu Q, Hao L, Shen Q, et al. CaMK II inhibition attenuates ROS dependent necroptosis in acinar cells and protects against acute pancreatitis in mice. Oxid Med Cell Longev 2021;2021:4187398.
76. Xiao J, Lin H, Liu B, Jin J. CaMKII/proteasome/cytosolic calcium/cathepsin B axis was present in tryspin activation induced by nicardipine. Biosci Rep 2019;39:BSR20190516.
77. Dawra R, Ku YS, Sharif R, et al. An improved method for extracting myeloperoxidase and determining its activity in the pancreas and lungs during pancreatitis. Pancreas 2008;37:62–68.
78. Wildi S, Kleeff J, Mayerle J, et al. Suppression of transforming growth factor beta signalling aborts caerulein induced pancreatitis and eliminates restricted stimulation at high caerulein concentrations. Gut 2007;56:685–692.
79. Gukovsky I, Cheng JH, Nam KJ, et al. Phosphatidylinositide 3-kinase gamma regulates key pathologic responses to cholecystokinin in pancreatic acinar cells. Gastroenterology 2004;126:554–566.

Received October 9, 2024. Accepted August 26, 2025.

Correspondence
Address correspondence to: Wu Luo, PhD, Medical Research Center, the First Affiliated Hospital, Wenzhou Medical University, Wenzhou, Zhejiang, China. e-mail: wuluo@wmu.edu.cn; Guang Liang, PhD, Medical Research Center, the First Affiliated Hospital, Wenzhou Medical University, Wenzhou. e-mail: wzmcliangguang@163.com; or Xin Liu, PhD, Department of Pharmacy and Institute of Inflammation, Zhejiang Provincial People's Hospital, Affiliated People's Hospital of Hangzhou Medical College, Hangzhou, Zhejiang, China. e-mail: 674888206@qq.com.

Acknowledgments
The authors thank the Scientific Research Center of Wenzhou Medical University for consultation and instrument availability that supported this work. The authors also thank MJEditor (www.mjeditor.com) for linguistic assistance of the manuscript. The Graphical Abstract and Schematic illustrations were created by BioRender (https://www.biorender.com/).

CRediT Authorship Contributions
Yi Fang (Data curation: Equal; Formal analysis: Lead; Investigation: Lead; Methodology: Lead; Writing – original draft: Lead; Writing – review & editing: Equal)
Xiang Hu (Data curation: Equal; Formal analysis: Equal; Investigation: Supporting; Methodology: Supporting; Supervision: Equal)
Lijun Ji (Data curation: Equal; Formal analysis: Equal; Investigation: Supporting; Methodology: Equal)
Jiaxi Ye (Investigation: Supporting; Methodology: Supporting)
Yaqian Cui (Investigation: Supporting; Methodology: Supporting)
Yongqiang Xiong (Data curation: Supporting; Investigation: Supporting)
Tianyang Jin (Data curation: Supporting; Investigation: Supporting)
Qingsong Zheng (Investigation: Supporting; Methodology: Supporting)
Guang Liang (Conceptualization: Equal; Funding acquisition: Equal; Project administration: Equal; Supervision: Equal; Writing – review & editing: Equal)
Xin Liu (Formal analysis: Equal; Funding acquisition: Supporting; Investigation: Equal; Project administration: Equal; Supervision: Equal)
Wu Luo (Conceptualization: Equal; Funding acquisition: Equal; Project administration: Equal; Supervision: Lead; Writing – original draft: Equal; Writing – review & editing: Lead)

Conflicts of interest
The authors disclose no conflicts.

Funding
This study was supported by the National Key Research Project (2017YFA0506000 to Guang Liang), National Natural Science Foundation of China (21961142009 to Guang Liang, 82300589 to Xin Liu), Natural Science Foundation of Zhejiang Province (LY22H070004 to Wu Luo), Medical and Health Research Project of Zhejiang Province (2024KY1271 to Wu Luo), and Zhejiang Provincial Key Scientific Project (2021C03041 to Guang Liang).